

PHYSICS

CHEMISTRY  
BIOLOGY

ENGINEERING

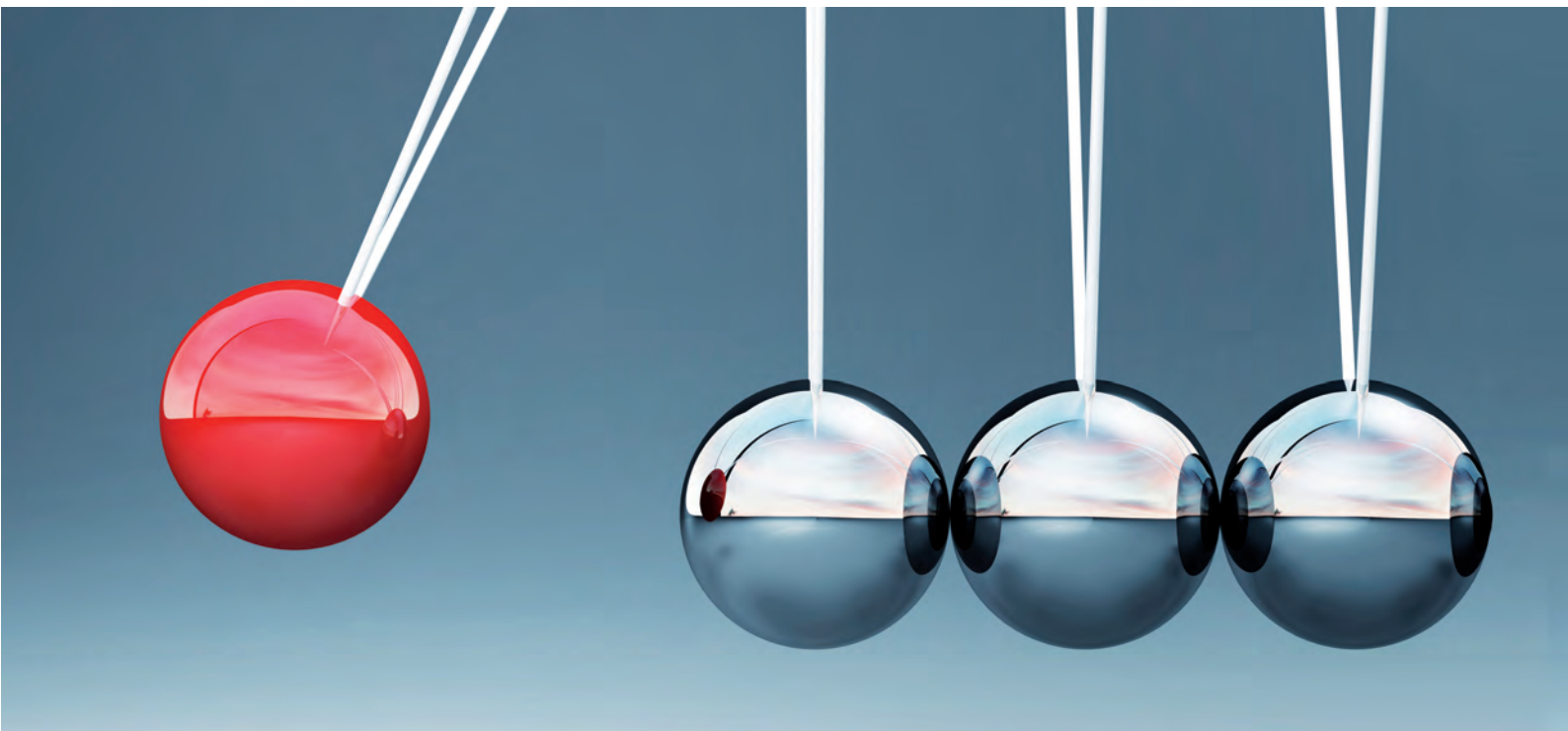


LD DIDACTIC

P5.8.5.5

# Helium Neon Laser

4747104 EN



**LEYBOLD®**





## Laser Sicherheitshinweise

Hiermit erklärt die Firma LD Didactic GmbH,  
dass es sich bei dem angebotenen Lasersystem um einen Aufbau handelt, der sowohl in  
Komponenten als auch im fertigen Aufbau einem Laser der Klasse 3A, 3B oder 4 nach DIN EN 60  
825-1 entspricht. Typischerweise ist die Pumpdiode eine Nd:YAG Laser Klasse 4, ein HeNe Laser mit  
Auskoppler Klasse 3A, aber ein HeNe mit zwei hochreflektierenden Spiegeln nur Klasse 1. Bitte die  
Anleitung oder Aufkleber beachten.

Aus Haftungsgründen dürfen diese Geräte oder Gerätesammlungen nicht an Privatleute verkauft  
werden. Der Einsatz von Lasern oberhalb Klasse 2 an allgemeinbildenden Schulen ist in  
Deutschland nicht gestattet.

Gewerbliche Abnehmer, Schulen und Universitäten werden hiermit darauf hingewiesen, dass aus dem  
missbräuchlichen Betrieb der Geräte ein Verletzungsrisiko, speziell für die Augen, resultiert.

Dem Benutzer obliegt insbesondere:

- Die relevanten Unfallverhütungsvorschriften zu beachten, zur Zeit beispielsweise BGV B2 und BGI 832
  - die OstrV zu beachten „Verordnung zum Schutz der Beschäftigten vor Gefährdungen durch künstliche optische Strahlung“
  - Der Betrieb der Geräte muss rechtzeitig beim Gewerbeaufsichtsamt und der Berufsgenossenschaft angezeigt werden.
  - Der Betreiber muss schriftlich einen Laserschutzbeauftragten benennen, der für die Einhaltung der Schutzmaßnahmen verantwortlich ist.
  - Die Geräte sind nur für den Betrieb in umschlossenen Räumen vorgesehen, deren Wände die Ausbreitung des Laserstrahls begrenzen.
  - Der Laserbereich ist deutlich und dauerhaft zu kennzeichnen.
  - Ab Laserklasse 4 ist eine Laser-Warnleuchte am Raumzugang notwendig.
  
  - Die Geräte sind zur Lehre und Ausbildung in Berufsschulen, Universitäten oder ähnlichen Einrichtungen gedacht.
  - Die Geräte nur innerhalb der in den Anleitungen vorgegebenen Betriebsbedingungen betreiben.
  - Die Geräte nur von entsprechend unterwiesenen Mitarbeitern und Studierenden benutzen lassen.
- Bei Handhabung des Gerätes durch Studenten müssen diese von entsprechend geschultem Personal überwacht werden.



Als praktische Ratschläge:

- Vor dem Einschalten auf Beschädigungen prüfen
- Nicht in den Strahl blicken
- Den Laserstrahl so führen, dass sich keine Personen, Kinder oder Tiere ungewollt im Strahlbereich befinden können
- Den Laserstrahl nicht auf reflektierende Flächen oder in den freien Raum richten
- Nicht mit reflektierenden Gegenständen im Laserstrahl arbeiten
- Armbanduhr, Schmuck und andere reflektierende Gegenstände ablegen.
- Beim Einsetzen optischer Bauteile den Laserstrahl an der Quelle abschalten oder geeignet abdecken, bis die Bauteile positioniert sind
- Teilweise wird mit unsichtbaren Laserstrahlen gearbeitet, deren Verlauf nicht sichtbar ist.
- Falls nötig, Laserschutzbrillen oder Laserjustierbrillen benutzen.

Die Firma LD Didactic GmbH haftet nicht für eine missbräuchliche Verwendung der Geräte durch den Kunden.

Der Kunde verpflichtet sich hiermit die Geräte nur entsprechend der rechtlichen Grenzen einzusetzen und insbesondere den Laserstrahl nicht im Straßenverkehr oder Luftraum zu verwenden oder in anderer Form auf Personen und Tiere zu richten.

Der Kunde bestätigt, das er befugt ist, diesen Laser zu erwerben und zu verwenden.

PHYSICS

CHEMISTRY  
BIOLOGY

ENGINEERING



## Laser Safety Notes

LD Didactic GmbH informs the customer this is laser equipment of either class 3A, 3B or 4 according to IEC 60 825. Typically a Nd:YAG Pump Diode is class 4, a HeNe with output coupler class 3A, but a HeNe with two high reflecting mirrors only class 1. Please see manual or attached labels for the exact specification of the laser.

Special safety precautions are necessary. Please check with local regulations. Typically the use requires a safety sign and a warning lamp that is on when the laser is activated and it might also be necessary to do and document a risk assessment.

Due to product liability, the laser must not be sold to individual persons. Companies, higher schools and universities might use it, but are notified that misuse of the laser poses a health risk, especially for the eyes.

The intended use of this equipment is for lessons, education and research in higher schools, universities or similar institutions.

Do not operate the devices outside parameters specified in the manual.

People using the laser must be properly trained and students must be supervised.

As a general guidance, the user is advised to:

- Check the laser for damages before use
- Not to look into the beam
- Take necessary measures that no people or animals can accidentally enter the beam area
- do not direct the beam on reflecting surfaces or into public areas
- do not work close to the light path with reflecting tools
- take off all jewelry and wristwatches when working with the laser to avoid reflections
- While placing or removing optical parts in the light path, switch off the laser or cover its exit
- Some of the experiments use invisible laser beams, but still might hurt the eye
- use laser protection glasses or laser adjustment glasses where necessary
- supervise students by trained personnel when they work with the laser system
- use the laser system only as described in the instruction manuals

Customer acknowledges the receipt of this information.

The customer indemnifies LD Didactic from liability for any damages that occur because of misuse of the laser.

The customer confirms that he will obey all local regulations and is allowed by law to buy and use the laser system.



# Table of Contents

<b>1.0 INTRODUCTION</b>	<b>4</b>
<b>2.0 FUNDAMENTALS</b>	<b>4</b>
2.1 <i>He-Ne energy- level diagram</i>	4
2.2 <i>Amplification</i>	6
2.3 <i>Resonators</i>	8
2.4 <i>Laser tubes and Brewster's windows</i>	9
2.5 <i>Wavelength selection</i>	10
2.5.1 Littrow prism	10
2.5.2 Birefringent crystal	10
2.5.3 Jones Matrix Formalism	10
2.6 <i>Mode selection</i>	13
2.7 <i>Bibliography</i>	13
<b>3.0 EXPERIMENT</b>	<b>14</b>
3.1 <i>Optical stability</i>	14
3.2 <i>Gaussian beams</i>	14
3.2.1 Measurements	15
3.3 <i>Output power</i>	15
3.4 <i>Mode structure</i>	16
3.5 <i>Wavelength selection</i>	16
3.5.1 Dispersive elements (prisms).	16
3.5.2 Diffractive elements	16
3.5.3 Interfering elements	16
3.5.4 Elements sensitive to polarisation	16
3.5.5 Littrow prism	16
3.5.6 Birefringent crystal	16
3.6 <i>Single mode operation with Etalon</i>	17
3.7 <i>Operation with infrared lines</i>	17
<b>4.0 SET-UP AND DESCRIPTION OF COMPONENTS</b>	<b>18</b>
4.1 <i>Description of the modules</i>	18
4.2 <i>Basic alignment</i>	20
4.3 <i>Alignment of the birefringent Tuner</i>	23
4.4 <i>Alignment of the Littrow Prism Tuner</i>	24
4.5 <i>Alignment of the Fabry-Perot Etalon</i>	25
4.6 <i>The high voltage controller ED-0070</i>	25
4.7 <i>Examples of measurements</i>	26

## 1.0 Introduction

The Helium-Neon laser was the first continuous laser. It was invented by Javan et. al. in 1961. Nowadays lasers are usually pre-adjusted using a He-Ne laser. But how did Javan manage to do this? This shows that it is no coincidence that Javan's first He-Ne laser oscillated at a wavelength of 1.5  $\mu\text{m}$ , since the amplification at this wavelength is considerably higher than the 632 nm line which is reached at what is now commonly known as the red line, which was made to oscillate only one year later by White and Ridgen. The similarity between the manufacturing techniques of He-Ne lasers and electron valves helped in the mass production and distribution of He-Ne lasers. The replacement of tubes by transistors in the sixties left a sufficiently redundant production capacity. In Germany for example, the Siemens tube factory took over this production and has produced over one million He-Ne lasers to date.

It is now clear that He-Ne lasers will have to increasingly compete with laser diodes in the future. But He-Ne lasers are still unequalled as far as beam geometry and the purity of the modes are concerned. Laser diodes will have to be improved to a great extent before they pose a serious threat to He-Ne lasers.

## 2.0 Fundamentals

### 2.1 He-Ne energy- level diagram

The fascination for inert gases and their clear atomic structure formed the basis for many spectroscopic investigations. The knowledge obtained through spectroscopic data was extremely helpful in deciding to choose helium and neon for the first lasers, using Schawlow Towne's discovery of lasing conditions in 1958 to estimate whether an inversion was feasible in laser operation. The lifetime of the s- and p-states were well known. Those of the s-states were longer than those of the p-states by a factor of about 10. The inversion condition was therefore fulfilled.

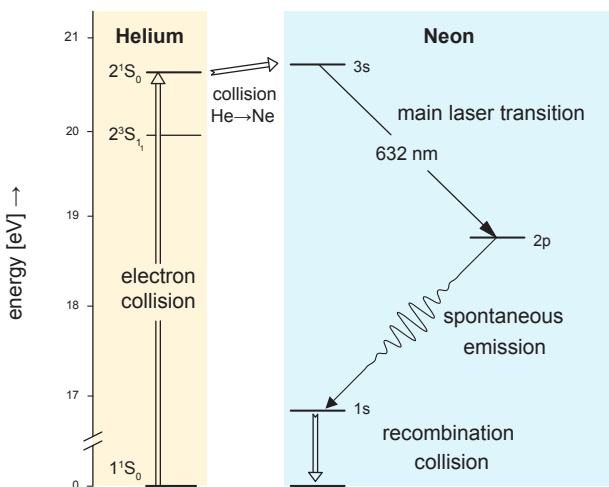


**Fig. 1: Excitation and Laser process for the visible Laser emission**

Fig. 1 shows the reduced energy-level diagram for helium and neon. Only those levels important in the discussion of the excitation and laser processes at a wavelength of 632 nm are indicated.

The left side of the representation shows the lower levels of the helium atoms. Observe how the energy scale is interrupted and that there is a larger difference in energy in the recombination process than is evident in the diagram. Paschen's names for the neon energy levels are used (Racah's term descriptions are often found as well). The terms are simply numbered consecutively, from bottom to top. A characteristic of helium is that its first states to be excited,  $2^1S_1$  and  $2^1S_0$  are metastable, i.e. optical transitions to the ground state  $1^1S_0$  are not allowed, because this would violate the selection rules for optical transitions. As a result of gas discharge, these states are populated by electron collisions (collision of the second type, Fig. 2). A collision is called a collision of the second type if one of the colliding bodies transfers energy to the other so that a transition from the previous energy state to the next higher or lower takes place. Apart from the electron collision of the second type there is also the atomic collision of the second type. In the latter, an excited helium atom reaches the initial state because its energy has been used in the excitation of a Ne atom. Both these processes form the basis for the production of a population inversion in the Ne system.

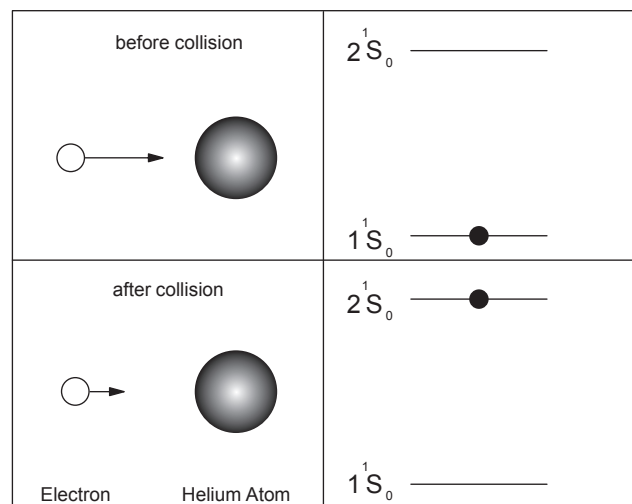


**Fig. 2: Electron collision of the second kind**

If we look at Fig. 1 we can see that the  $2^1S_0$  is slightly below the 3s level of the neon. However, the additional thermal energy  $kT$  is sufficient to overcome this gap. As already mentioned, the lifetime of the s-states of the neon are approximately 10 times longer as those of the p-states. An immediate population inversion between the 3s and the 2p levels will therefore be generated. The 2s level is emptied due to spontaneous emission into the 1s level. After this the neon atoms reaching their ground state again, primarily through collisions with the tube wall (capillary), since an optical transition is not allowed. This calming down process is the bottle neck in the laser cycle. It is therefore advisable to choose a capillary diameter that is as small as possible. However, the laser will then suffer more losses. Modern He-Ne lasers work at an optimum of these contradictory conditions. This is the main reason for the comparatively low output of He-Ne lasers.

We have discussed the laser cycle of the commonly known red line at 632 nm up to this point. However the neon has several other transitions, used to produce about 200 laser

lines in the laboratories. The following explanation describes the energy-level diagram for further visible lines. After that infrared laser transitions will be discussed.

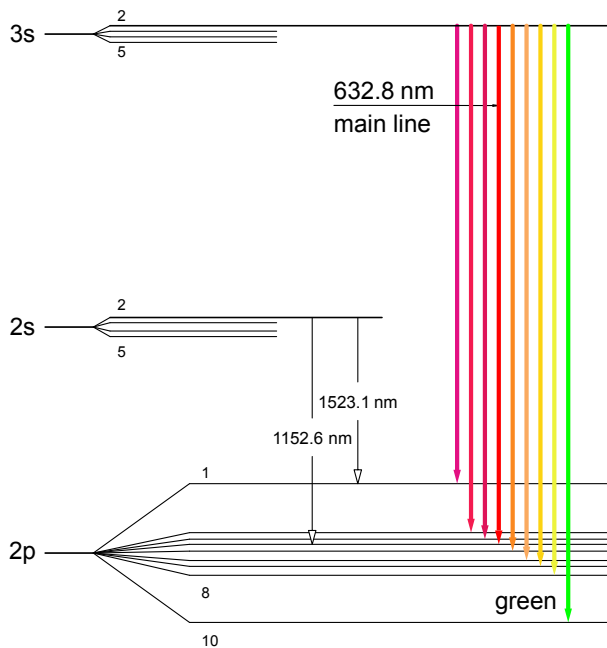


**Fig. 3: The most important laser transitions in the neon system**

The 3s state is populated by Helium atoms of the  $2^1S_0$  state as a result of an atomic collision. The 3s state consists of 4 sub-states out of which it is primarily the  $3s_2$  state which has been populated through the collision process. The population density of the other 3s sub-states is app. 400 times less than that of the  $3s_2$  state. The 2s state is populated by the Helium atoms of the  $2^3S_1$ , as a result of an atomic collision.

The four sub-states of the 2s group are all populated in a similar way. Visible (VIS) optical transitions and laser processes are taking place between the  $3s_2 \rightarrow 2p_i$  and infrared (IR) between the  $2s_i \rightarrow 2p_i$  energy levels.

The Table 1 shows the most important laser transitions. The Einstein coefficients  $A_{ik}$  are given for the visible lines and amplification is indicated as a percentage per meter.

Further laser transitions are known, which start at the  $3s_2$  level and terminating at the  $3p$  level of the neon. However, these laser transitions lie even further within the infrared spectral range and cannot be detected with the silicon detector used in the experiment. They are not particularly suitable for experiments. Notice that these lines are originating from the same level as the visible lines and are therefore competing with them.

Since the cross-section of the stimulated emission is increasing with  $\lambda^3$  as well, the amplification of these lines is therefore very strong. This applies to the  $3.39 \mu\text{m}$  line in particular, which, due to a sufficiently long capillary, shows laser activity (so called super fluorescence) even without an optical resonator.

Transition	Wavelength [nm]	$A_{ik} [10^8 \text{ s}^{-1}]$	Gain [%/m]	
$3s_2 \rightarrow 2p_1$	730.5	0,00255	1,2	①
$3s_2 \rightarrow 2p_2$	640.1	0,0139	4,3	①
$3s_2 \rightarrow 2p_3$	635.2	0,00345	1,0	①
$3s_2 \rightarrow 2p_4$	632.8	0,0339	10,0	①
$3s_2 \rightarrow 2p_5$	629.4	0,00639	1,9	①
$3s_2 \rightarrow 2p_6$	611.8	0,00226	1,7	①
$3s_2 \rightarrow 2p_7$	604.6	0,00200	0,6	
$3s_2 \rightarrow 2p_8$	593.9	0,00255	0,5	
$3s_2 \rightarrow 2p_9$	Transition not allowed			
$3s_2 \rightarrow 2p_{10}$	543.3	0,00283	0,52	
$2s_2 \rightarrow 2p_1$	1523.1			③
$2s_2 \rightarrow 2p_2$	1177.0			②
$2s_2 \rightarrow 2p_3$	1160.5			
$2s_2 \rightarrow 2p_4$	1152.6			②
$2s_2 \rightarrow 2p_5$	1141.2			②
$2s_2 \rightarrow 2p_6$	1084.7			②
$2s_2 \rightarrow 2p_7$	1062.3			
$2s_2 \rightarrow 2p_8$	1029.8			
$2s_2 \rightarrow 2p_9$	Transition not allowed			
$2s_2 \rightarrow 2p_{10}$	886.5			
$2s_3 \rightarrow 2p_2$	1198.8			②
$2s_3 \rightarrow 2p_5$	1161.7			②
$2s_3 \rightarrow 2p_7$	1080.1			②

**Table 1: Transitions and Laser lines**

- ① Laser transition is demonstrated provided set of mirrors
- ② Laser transitions are demonstrated in the experiment with optional IR mirror set
- ③ Laser transitions are demonstrated with special mirror set

Appropriate measures must be taken to suppress the super fluorescence to avoid a negative influence on the visible laser lines.

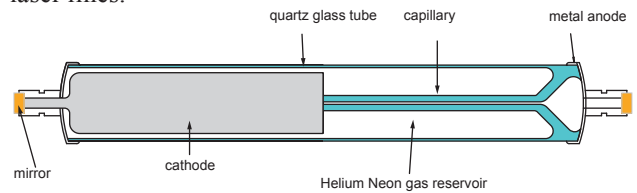


**Fig. 4: Modern He-Ne laser with glass-to-metal soldering of the anode, cathode and laser mirror**

Fig. 4 shows a modern laser tube made with highly perfected manufacturing techniques and optimised to suit the physical aspects of the laser. This applies to the resonator in particular, which is designed for a best possible output in the fundamental mode with a purely Gaussian beam and spectral purity in single mode operation (e.g. for interferometric length measurement). The fulfilment of this demand depends, amongst other aspects, on the optimal adaptation of the resonator to the amplification profile of the Neon. The behaviour of Neon during amplification will therefore be discussed first.

## 2.2 Amplification

The Neon atoms move more or less freely in the laser tube but at different speeds. The number  $N$  of neon atoms with the mass  $m$ , within a speed interval of  $v$  to  $v+dv$  is described according to the Maxwell-Boltzmann distribution Fig. 5.

$$\frac{n(v)}{N} = \frac{4}{\sqrt{\pi}} \cdot \frac{v^2}{\sqrt{(2kT/m)^2}} \cdot e^{-\frac{mv^2}{kT}} dv$$

$T$  is the absolute temperature and  $k$  Boltzmann's constant. The above equation is applicable for all directions in space. However, we are only interested in the distribution of speed in the direction of the capillary. Using  $v^2 = v_x^2 + v_y^2 + v_z^2$  we obtain for the direction  $x$ :

$$\frac{n(v_x)}{N} = \sqrt{\frac{m}{2kT}} \cdot e^{-\frac{m \cdot v_x^2}{2kT}} dv_x \quad \text{Eq. 2.1}$$

A resting observer will now see the absorption or emission frequency shifted, due to Doppler's effect (Ch. Doppler: Abh. d. K. Boehmischen Ges. d. Wiss. (5). Vol. II (1842) P.465), and the value of the shift will be:

$$v = \frac{v_0}{1 \pm v/c} \quad \text{assuming } v \ll c \quad \text{Eq. 2.2}$$

$v_0$  is the absorption or emission frequency of the resting neon atom and  $c$  the speed of light. If the Doppler equation (Eq. 2.1) is used to substitute the velocity  $v$  in the Maxwell-Boltzmann's velocity distribution (Eq. 2.2) the line broadening produced by the movement of Neon atoms can be found. Since the intensity is proportional to the number of absorbing or emitting Neon atoms, the intensity distribution will be:

$$I(v) = I(v_0) \cdot e^{-\left(c \cdot \frac{v-v_0}{v_0 \cdot v_w}\right)^2} \quad \text{Eq. 2.3}$$

$v_w$  is the most likely speed according to:

$$v_w = \sqrt{\frac{2kT}{m}}$$

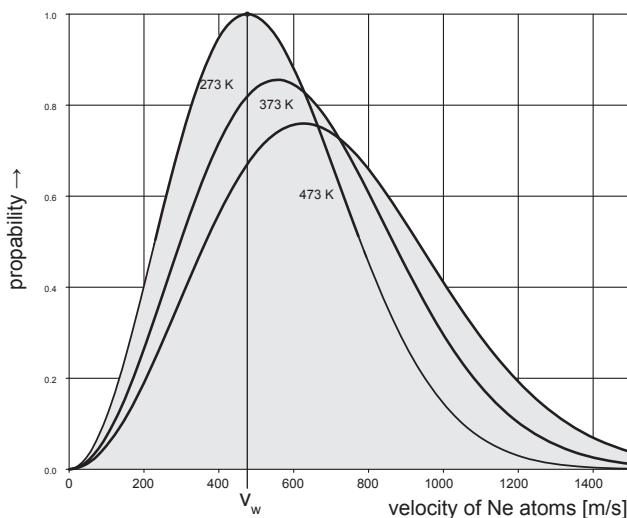


Fig. 5: Probability Distribution for the velocity  $v$  of the neon atoms within the interval  $v$  to  $v + dv$ .

The full width at half maximum is calculated by setting  $I(v) = 1/2 I(v_0)$  and the result is:

$$\Delta v_{\text{Doppler}} = \sqrt{4 \cdot \ln 2} \cdot \frac{v_w}{c} \cdot v_0 \quad \text{Eq. 2.4}$$

We can conclude from Eq. 2.4 that the line broadening caused by Doppler's effect is larger in the case of:

- higher resonance frequencies  $v_0$
- or smaller wavelengths ( $v_0 = c/\lambda_0$ , UV - lines)
- higher most likely velocity  $v_w$
- that means higher temperature  $T$

and smaller in the case of:

- a larger particle mass.

The line profile also corresponds to a Gaussian distribution curve (Eq. 2.3). Fig. 6 shows this kind of profile. The histogram only approaches the distribution curve when the speed intervals  $dv$  are small.

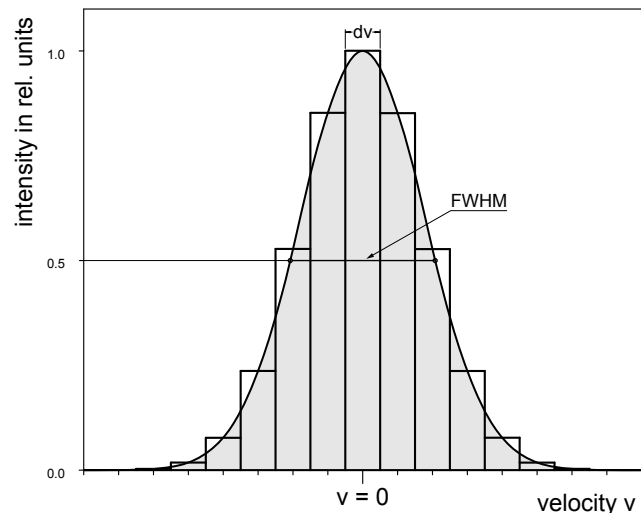


Fig. 6: Inhomogeneous line profile, speed intervals  $dv$

Why these speed intervals  $dv$  or frequency intervals  $dv$  you may ask. Actually there are formal reasons for this. Not having any intervals at all would be like wanting to make a statement on fishing out a particle with an exact speed or frequency from the ensemble. It is almost impossible to do. So, we define finite probabilities of ensembles by using intervals. If we succeed in this, we can make the intervals smaller and work with "smooth curves".

On closer observation we can see that a line broadened by the Doppler effect actually does not have a pure Gaussian distribution curve.

To understand this, we pick out an ensemble of Ne atoms whose speed components have the value  $v$  in the direction we are looking at. We expect that all these atoms emit light with the same frequency  $\nu$  or wavelength  $\lambda$ . But we have to consider an additional effect which is responsible for the natural line width of a transition. We know that each energy level poses a so called life time. The population  $n_2$  of a state 2 decays into a state 1 with lower energy with a time constant  $\tau_s$  following the equation :

$$n_2(t) = n_2(t=0) \cdot e^{-A_{21} \cdot t} \quad \tau_s = \frac{1}{A_{21}}$$

$A_{21}$  is the famous Einstein coefficient for the spontaneous emission. The emission which takes place is termed as spontaneous emission.

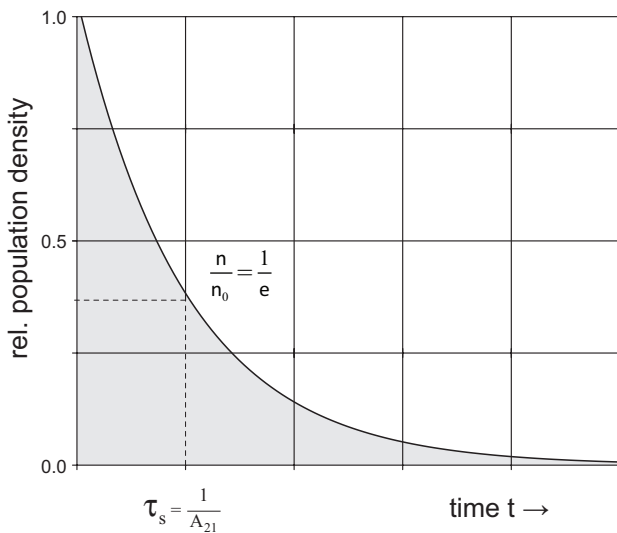


**Fig. 7: Decay of the population of state 2 into a state 1 with lower energy**

This shows us, that the ensemble of Ne atoms does not emit light at a single frequency. It emits a frequency spectra represented by an Lorentz profile (Fig. 8).

$$\delta(\nu) = \frac{1}{4\pi \cdot (\nu - \nu_{21})^2 + (1/2 \cdot \tau_s)^2}, \nu_0 \equiv \nu_{21}$$

The exact profile formation can be determined from the convolution of the Gaussian profile with the individual Lorentz profiles. The result obtained in this manner is called as the Voigt profile. Since one group of particles in an ensemble can be assigned to a given speed  $v$ , these groups have characteristics that differentiate them. Every group has its own frequency of resonance. Which group a photon interacts with depends on the energy (frequency) of the photon. This does not affect the other groups which are not resonant on this interaction. Therefore such kind of a gain profile is termed inhomogeneous.

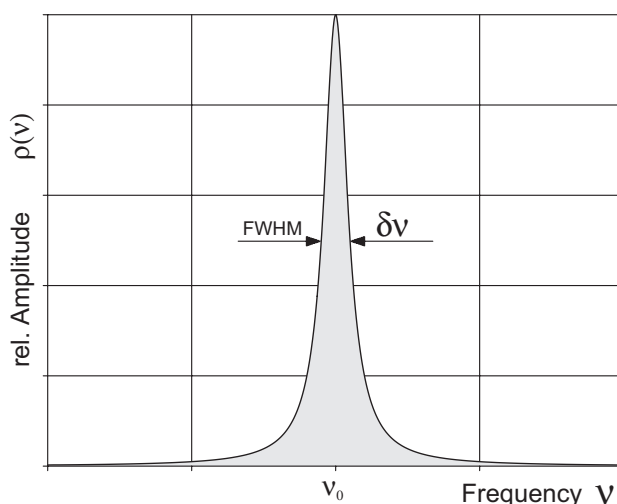


**Fig. 8: Natural linewidth (FWHM) caused by spontaneous emission**

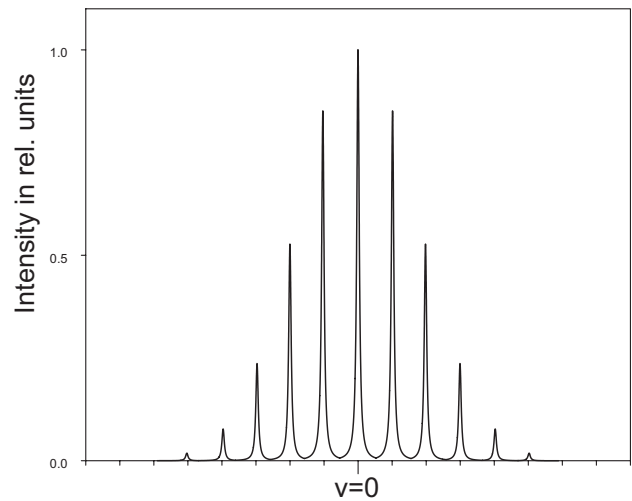


**Fig. 9: Natural broadened line profiles (homogeneous) for groups of speed  $v$  within the inhomogeneous Doppler broadened gain profile**

As we already know gain occurs in a medium when it shows inversion. This means that the population density of the upper level  $n_2$  (3s in the Ne-system) is larger than the population density of the lower state  $n_1$  (2p). In Fig. 10 the population profiles are rotated by 90° to draw them in the well known energy level diagram. Transition can only take place between sub-ensembles which have the same velocity  $v$  because the optical transition does not change the speed of the particular Ne atom.

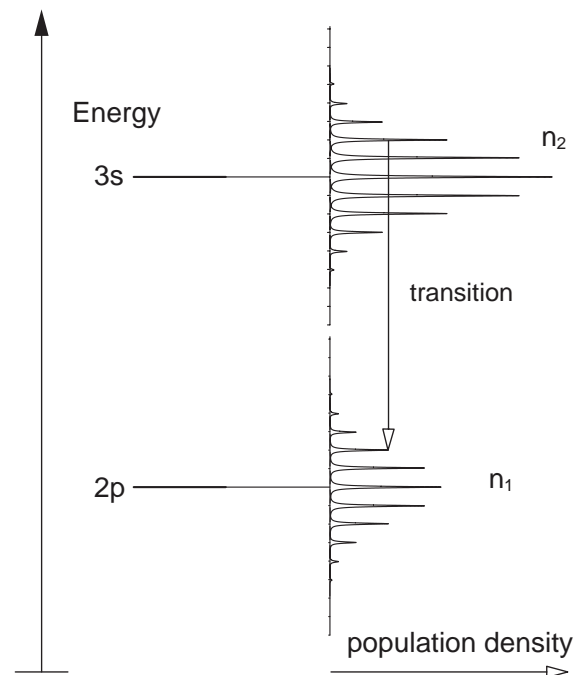


**Fig. 10: Population inversion and transition between sub-ensembles with same velocity  $v$**

The situation of Fig. 10 shows a population inversion  $n_2 > n_1$ . Besides some specific other constants the gain is proportional to the difference  $n_2 - n_1$ . Now we will place the inverted ensemble of Ne atoms into an optical cavity, which is formed by two mirrors having the distance of  $L$ . Due to the spontaneous emission photons are generated which will be amplified by the inverted medium and reflected back from the mirrors undergoing a large number of passes through the amplifying medium. If the gain

compensates for the losses, a standing laser wave will be built up inside the optical resonator. Such a standing wave is also termed as oscillating mode of the resonator also eigenmode or simply mode. Every mode must fulfil the following condition:

$$L = n \cdot \frac{\lambda}{2} \text{ or } L = n \cdot \frac{c}{2\nu}$$

L represents the length of the resonator,  $\lambda$  the wavelength, c the speed of light,  $\nu$  the frequency of the generated light and n is an integer number. Thus every mode has its frequency of

$$\nu(n) = n \cdot \frac{c}{2L}$$

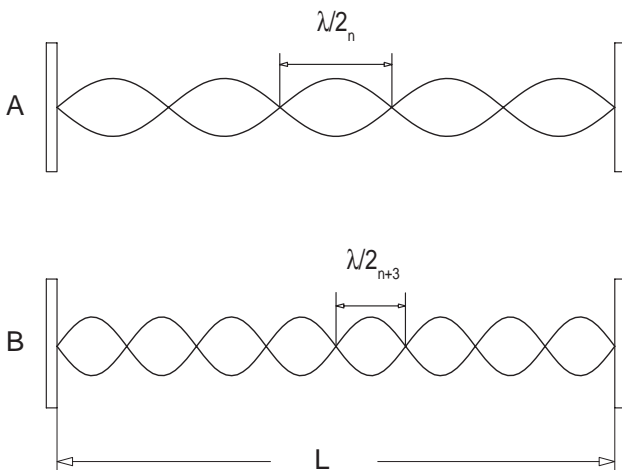


**Fig. 11: Standing longitudinal waves in an optical resonator. A with n nodes and B with n+3 nodes**

e.g. A He-Ne-Laser with a resonator length of 30 cm at an emission wavelength  $\lambda$  of 632.8 nm will have the following value for n:

$$n = \frac{\nu}{c} \cdot 2 \cdot L = 2 \cdot \frac{L}{\lambda} = 2 \cdot \frac{0,3}{632,8 \cdot 10^{-8}} = 949.167$$

The difference in frequency of two neighboured modes is:

$$\Delta\nu = \nu(n+1) - \nu(n) = (n+1) \cdot \frac{c}{2L} - n \cdot \frac{c}{2L} = \frac{c}{2L}$$

In the above example the distance between modes would be

$$\Delta\nu = \frac{3 \cdot 10^8}{2 \cdot 0,3} = 5 \cdot 10^8 \text{ Hz} = 500 \text{ MHz}$$

If the active laser material is now brought into the resonator standing waves will be formed due to the continuous emission of the active material in the resonator and energy will be extracted from the material. However, the resonator can only extract energy for which it is resonant. Strictly speaking, a resonator has an indefinite amount of modes, whereas the active material only emits in an area of frequency determined by the emission line width.

Fig. 12 shows the situation in the case of material that is

inhomogeneously broadened.

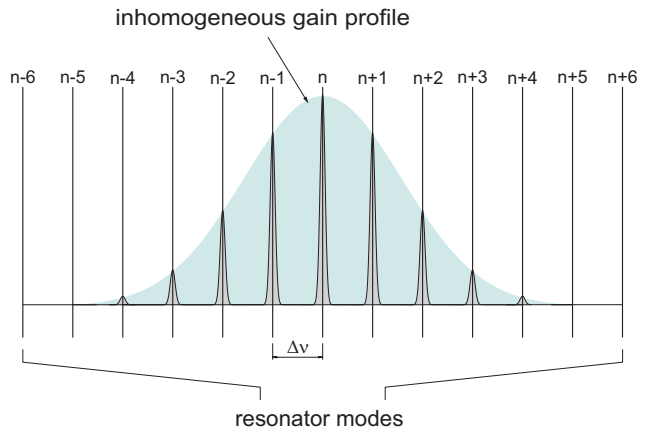


**Fig. 12: Inhomogeneously broadened gain profile (Gaussian profile) interacting with an optical resonator**

If the laser is operating in a stationary state, we can see that it is emitting several longitudinal modes. These are exactly the same modes that will be found in the emission profile. Since the modes are fed by an inhomogeneous emission profile they can also exist independently. The He-Ne-Laser is a classic example of this.

### 2.3 Resonators

In the following section some fundamentals used in the description and calculation of optical resonators will be introduced. Stability diagrams, the beam radius and beam sizes for the resonator types used in later experiments will be calculated and discussed. The investigations and calculations will be carried out for an “empty” resonator since the characteristics of the resonator will be particularly influenced (e.g. thermal lenses, abnormal refractive index etc.). The ABCD law will be introduced and used in this context. Just like the Jones matrix formalism this type of optical calculation is an elegant method of following the beam (ray tracing) in a complex optical system. Fig. 13 shows that an identical lens system can be constructed for every optical resonator. The beam path of the resonator can be traced using the ABCD law, aided by an equivalent lens system. So, how does the ABCD law work ?

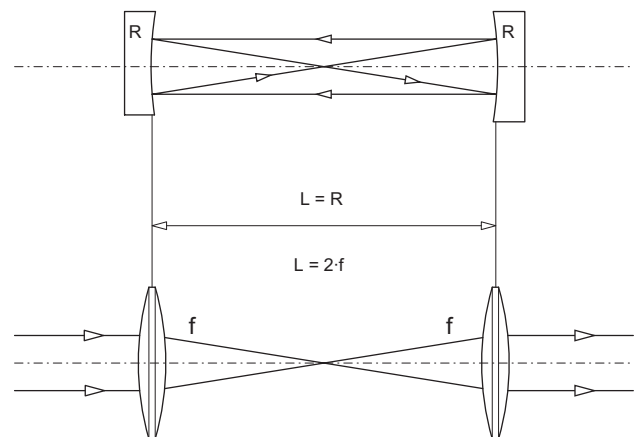


**Fig. 13: Spherical resonator with equivalent lens guide**

First we must presume that the following calculations are correct for the limits of geometric optics, that is if the beam angle is  $< 15^\circ$  to the optical axis, close to  $\sin \alpha \approx \alpha$ . This has been fulfilled in most systems, especially for laser

resonators. A light beam is clearly defined by its height  $x$  to the optical axis and the slope at this point (Fig. 14).

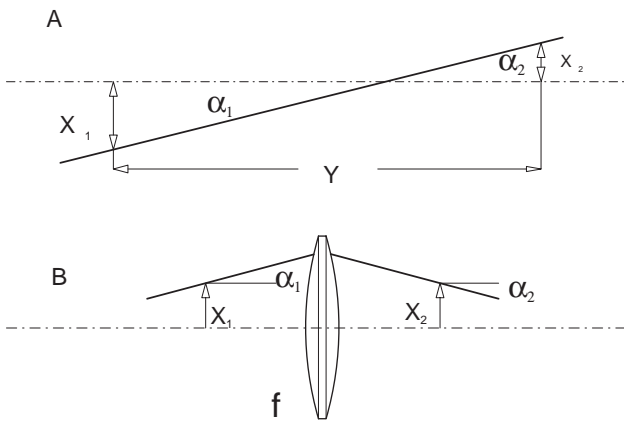


Fig. 14: (A) light beam with the characteristic parameters, (B) trace through a lens.

The matrix to be introduced is called the beam transfer matrix or ABCD matrix. When this matrix is applied to the input quantities  $x_1$  and  $\alpha_1$  the resulting output quantities will be  $x_2$  and  $\alpha_2$ :

$$\begin{pmatrix} x_2 \\ \alpha_2 \end{pmatrix} = \begin{pmatrix} A & B \\ C & D \end{pmatrix} \cdot \begin{pmatrix} x_1 \\ \alpha_1 \end{pmatrix}$$

Example A in Fig. 10 shows the free propagation of a beam, from which we can deduce that  $\alpha_1 = \alpha_2$  and  $x_2 = x_1 + \alpha_1 y$ . So, the ABCD matrix in this case is:

$$A = \begin{pmatrix} 1 & y \\ 0 & 1 \end{pmatrix}$$

In example B which shows a thin lens the matrix is:

$$B = \begin{pmatrix} 1 & 0 \\ -1/f & 1 \end{pmatrix}$$

It is easy to understand that the combination of example A and B is a result of free beam propagation with subsequent focusing with a thin lens

$$X_2 = A \cdot B \cdot X_1$$

A series of ABCD matrices for different optical elements can be drawn out with this method. They have been compiled by Kogelnik and Li [3]. The above examples are sufficient for the calculation of a resonator. Beams in an optical resonator have to pass through the same optical structure several times. After passing through it  $n$  times the ABCD law for a particular place  $Z$  of the lens guide (Fig. 13) would be:

$$\begin{pmatrix} x_f \\ \alpha_f \end{pmatrix}^n = \begin{pmatrix} A & B \\ C & D \end{pmatrix}^n \cdot \begin{pmatrix} x_i \\ \alpha_i \end{pmatrix}$$

In this case the ABCD matrix is the identical lens guide given to the resonator. The  $n$ -th power of a  $2 \times 2$  matrix is calculated as follows:

$$\begin{pmatrix} A & B \\ C & D \end{pmatrix}^n = \frac{1}{\sin(\theta)} \cdot \begin{pmatrix} a & b \\ c & d \end{pmatrix}$$

$$a = A \cdot \sin(n\theta) - \sin((n-1) \cdot \theta)$$

$$b = B \cdot \sin(n\theta)$$

$$c = C \cdot \sin(n\theta)$$

$$d = D \cdot \sin(n\theta) - \sin((n-1) \cdot \theta)$$

$$\theta = \arccos\left(\frac{A+D}{2}\right)$$

The trace of the above ABCD matrix  $|A+D|$  must be  $< 1$  if the beams are to remain within the lens guide.

$ A + D  \leq 1$	<b>Eq. 2.5</b>
------------------	----------------

This is now the criteria of stability for the lens guide and therefore also for the accompanying resonator.

Let us conclude.

An identical lens guide system can be allocated to every resonator. The ABCD matrix is determined for this optical structure (several simple lenses). The stability diagram for the different mirror intervals with given mirror radii is deduced using Eq. 2.5.

## 2.4 Laser tubes and Brewster's windows

Brewster windows function in two ways. They hermetically seal the tube, as well as ensuring that there is a definite polarisation in laser oscillation without additional losses.

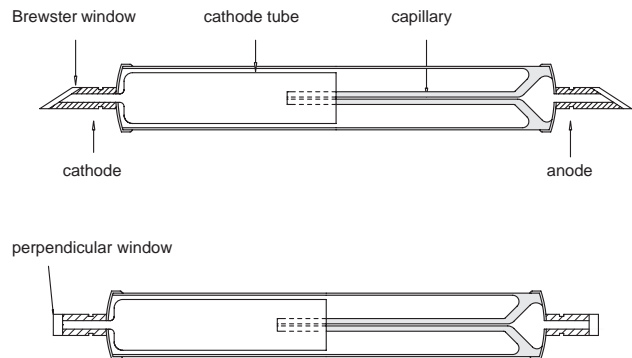
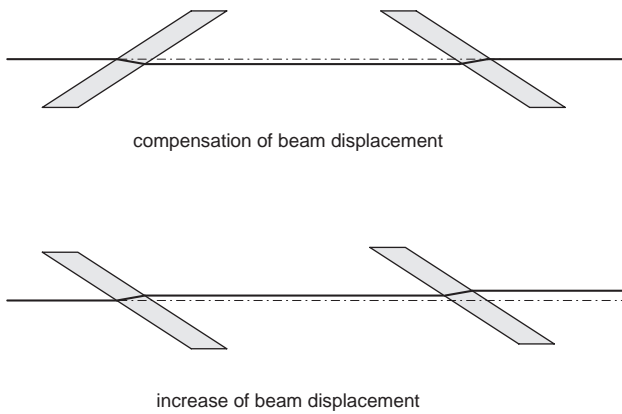


Fig. 15: Laser tube with Brewster's windows as used in the experiment and perpendicular windows with highly anti reflection coating

The discharge only burns in the capillary. This is ensured by the expansion and melting of the capillary with the glass tube. Brewster's windows are soldered on to a special metal (Vacon). The window flange on the anode side is made completely out of glass, to prevent coming into contact with the harmful high voltage during the required cleaning work. The tube needs an ignition voltage of approximately 8 kV and an operating voltage of about 2 kV. The optimal current for the 632 nm line is 5 mA.



**Fig. 16:** Two possible arrangements of Brewster windows. The one above compensates for displaced beams.

The Brewster windows of the laser tube are arranged in a way that enables compensation for beam displacement by the windows.

## 2.5 Wavelength selection

Lasers that are continuously variable from UV to IR, are probably the dream of every laser physicist. There has been a lot of research in this area and some goals have been partially achieved. e.g. The dye laser is a tunable laser, but it only covers a wavelength range of approx. 50 - 100 nm, depending on the dye used each time. The dye laser is being increasingly replaced by Titanium -Sapphire lasers which emit from dark red to IR. A birefringent filter is usually used in these systems as a tuning element, as described in 2.5.2. Both lasers require argon-ion lasers as a pump light source. This laser can oscillate on several lines. The tuning element in this case is a Littrow prism, as described below.

### 2.5.1 Littrow prism

Littrow's idea is simple, therefore it is also ingenious. He produced a prism in which the refractive angle is chosen in such a way that, in the arrangement of the minimal deviation (beam runs parallel to the hypotenuse), the beam enters the prism just under the Brewster's angle. In this way, there are minimal reflection losses. This kind of prism is also known as a Brewster's prism.

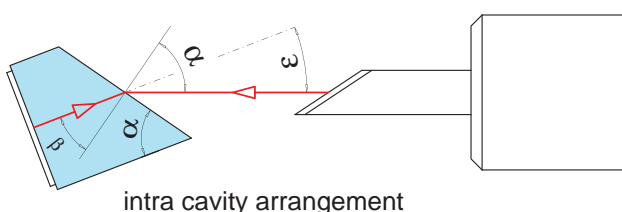
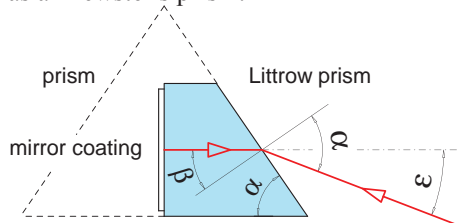


**Fig. 17:** Formation of a Littrow prism out of a Brewster's prism and its arrangement inside the resonator

Littrow then took the prism apart by cutting it down the middle and coated the surface with a highly reflecting substance. If the refractive index of the first layer is similar to the prism material, the Fresnel losses will be considerably reduced and the result will be an element suffering few losses, that can be used inside the resonator to select wavelengths.

### 2.5.2 Birefringent crystal

Birefringent crystals are indispensable in laser technology. They are used as optical retarder and also as tuning elements. At this point we will introduce a formalism describing the interaction between light and birefringent optics in a simple way. This formalism enables us to analyse and represent the way in which various birefringent components work, with regard to computer applications in particular.

### 2.5.3 Jones Matrix Formalism

Jones created the basis for this formalism in 1941. We should really be grateful to him. He was probably one of those people who didn't think much of exercises with complex numbers and sin and cos theorems.

The electric field intensity of light is usually represented in the vectorial form:

$$\vec{E} = \vec{E}_0 \cdot \sin(\omega t + \vec{k}\vec{r} + \delta)$$

$\vec{E}_0$  is the amplitude unit vector describing the size and direction (polarisation) of the electrical field

$\omega = 2 \pi \nu$ ,  $\nu$  is the frequency of light  
 $t$  is the time

$\vec{k}$  is the wave vector, containing the propagation direction and the wavelength  $\lambda$ :

$$|\vec{k}| = \frac{2\pi}{\lambda}$$

$\vec{r}$  is the displacement vector in the system of coordinates of the light wave

$$\delta = \frac{2\pi}{\lambda} |\vec{r}_1 - \vec{r}_2|$$

$\delta$  is a constant phase shift with respect either on a fixed coordinate or a fixed frequency

A complete description of a light wave still requires information on the magnetic field of the light wave. However, it need not be considered for most applications in the field of optics since the interaction of light with materials that do not absorb, is primarily of an electrical nature and not a magnetic one. As regards strictly theoretical derivations the magnetic field must fulfil certain conditions for continuity at the bordering surfaces. We do not propose to reflect on this aspect, however, and will therefore not discuss it any further at this point.

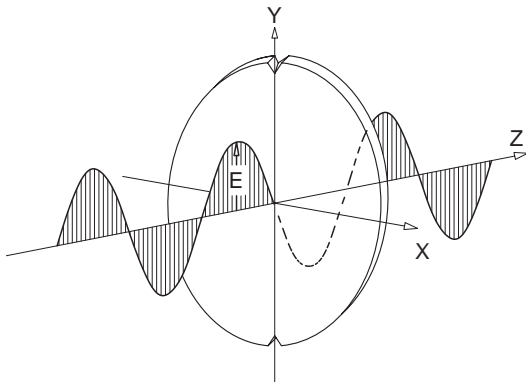


**Fig. 18: Passage of a light wave through an optical plate.**

The term “optical” is used to indicate that this plate has been manufactured for optical applications and that apart from characteristics specific to the material, the light wave has no outside obstacles (e.g. bubbles, impurities, etc.). The situation represented in Fig. 18 is typical for the use of birefringent components. It is therefore sufficient to be interested only in the X and Y components of the electrical field E. So, the light wave will be described by:

$$J = \begin{pmatrix} E_x \cdot e^{i\omega t} \\ E_y \cdot e^{i\omega t + \delta} \end{pmatrix} \quad \text{Eq. 2.6}$$

Since the frequency of the X and Y amplitude will always be the same and for power calculations fast oscillating terms will be neglected, we can simplify Eq. 2.6 to:

$$J = \begin{pmatrix} E_x \\ E_y \cdot e^{i\delta} \end{pmatrix}$$

Let us normalise the power P of the light wave to 1. Then

$$P = E_x^2 + E_y^2 = 1$$

It can easily be deduced that:

$$P = J J^{-1}$$

The minus sign in the J exponent means the conjugate complex of J (substitute i by -i). For a light wave that is polarised in the direction of the Y-axis it will be:

$$J = \frac{1}{\sqrt{2}} \cdot \begin{pmatrix} 0 \\ 1 \end{pmatrix}$$

In an analogous representation for a wave polarised in the direction of X the equation would be:

$$J = \frac{1}{\sqrt{2}} \cdot \begin{pmatrix} 1 \\ 0 \end{pmatrix}$$

We know that, based on the validity of the superposition principle of linear optics, any given number of polarised linear waves can be represented by the vectorial addition of two mutually perpendicular individual waves. By adding the two Jones vectors given above we would get linear polarisation of light oscillating at 45 degrees to the X or Y axis.

$$J = J_1 + J_2 = \frac{1}{\sqrt{2}} \begin{pmatrix} 1 \\ 0 \end{pmatrix} + \frac{1}{\sqrt{2}} \begin{pmatrix} 0 \\ 1 \end{pmatrix} = \frac{1}{\sqrt{2}} \begin{pmatrix} 1 \\ 1 \end{pmatrix}$$

If one component has a phase shift  $\delta$  with respect to the other component, the result will be elliptical polarised light. If the phase shift  $\delta$  is  $\lambda/4$  the result will be the circu-

lar polarisation of light.

$$\delta = \frac{2\pi}{\lambda} \cdot \Delta \quad , \quad \Delta = \frac{\lambda}{4} \Rightarrow \delta = \frac{\pi}{2}$$

The Jones vector for this kind of light has the following form.

$$J = \frac{1}{\sqrt{2}} \cdot \begin{pmatrix} 1 \\ i \end{pmatrix} \quad \text{note : } e^{i\frac{\pi}{2}} = i$$

An optical component which can produce such a phase shift is called “birefringent” or double refractive. An element which works selectively on one component only works as polariser. The difference between the two is that whereas the polariser removes a component, the birefringent plate slows one component down in relation to the other, in a way that the components differ in phase behind the plate. Before giving the Jones matrices for these elements we will explain briefly the way the elements work. A simple model will be used for this purpose. Light will be observed as an electromagnetic oscillation. We consider the optical component as a collection of many dipoles. These dipoles are determined by the type and form of the electron shells which each atom or molecule has. These dipoles are excited by the electromagnetic field of the light and are thus turned out of their equilibrium (susceptibility). The dipoles absorb energy of the light (virtual absorption) and send them out again. However, a dipole cannot send its beam in the direction of its own axis. If a crystal has two kind of dipoles, which are at a particular angle to each other, they can only emit and absorb light within the area of their angles. If the process of absorption and emission is slower in one kind of dipole than in the other there will be a phase shift. Macroscopically it seems as if there were a higher refractive index. A change in beam direction takes place because of the different dipole directions, i.e. there are two separate beam directions within the component. If a parallel light beam penetrates into this kind of material the result is, indeed, two beams leaving the crystal. In this case both beams are polarised perpendicularly to each other and have a phase shift between each other.

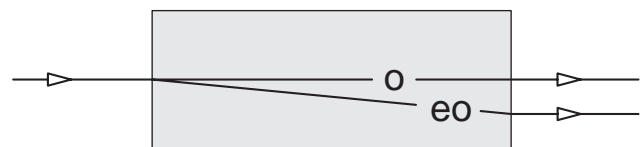


**Fig. 19: Birefringent crystal**

This phenomenon is called birefringence. These two marked directions of the crystal also have two distinctive refractive indices. Since one beam appears to be violating the Snell’s law, it is called extraordinary (eo) and the one behaving normally is ordinary (o). Crystal quartz and calcite are materials which behave in this way. There are also a series of other crystals but these two have proved successful in laser technology. Thin plates, used as optical retarder are mostly made out of quartz because it is hard enough for this purpose.

Mica sheets have also been used but they are not suitable for use inside the resonator because of the losses involved. Please note that only crystal quartz has a birefringent behaviour. Quartz that has already been melted (Quartz glass) loses this quality. A whole series of laser compo-

nents are made out of calcite [1]. Short calcite crystals are sufficient to produce the required beam separation, e.g. as with the active Q-switch, because of the great difference between the ordinary and extraordinary refractive indices. The Jones matrix formalism can now be applied in the description of the interaction of a light wave with such materials. Retarding plates and polariser can be represented as Jones matrices in the same way that a plane wave can be represented as a Jones vector. Polariser which allow X or Y polarised to pass are as follows:

$$P_x = \begin{pmatrix} 1 & 0 \\ 0 & 0 \end{pmatrix} \text{ and } P_y = \begin{pmatrix} 0 & 0 \\ 0 & 1 \end{pmatrix}$$

If the polariser is turned around the beam over the angle  $\theta$ , P must be treated with the transformation or rotational matrix:

$$R(\theta) = \begin{pmatrix} \cos(\theta) & \sin(\theta) \\ -\sin(\theta) & \cos(\theta) \end{pmatrix}$$

and the result for the turned polariser will be:

$$P(\theta) = R(-\theta) \cdot P \cdot R(\theta)$$

A birefringent plate whose optical axis runs parallel to the x or y axis has the following Jones matrix:

$$V = \begin{pmatrix} e^{-i\frac{\delta}{2}} & 0 \\ 0 & e^{i\frac{\delta}{2}} \end{pmatrix}$$

and has also to be transformed by the rotational matrix  $R(\theta)$  in case the optical axis of the crystal was rotated around the angle  $\theta$ . To prevent misunderstandings regarding the optical axes, we must point out that the optical axis of the crystal is the one in which the ordinary refractive index is effective. An account of an examination carried out with a  $\lambda/2$  plate using the Jones matrix formalism is given in [1]. A birefringent plate made out of crystal quartz is used in the He-Ne experimental laser for selecting the wavelengths. This kind of element is also known as a birefringent filter or birefringent tuner. This element was originally used to tune dye lasers. It was first successfully used in a He-Ne laser by this author [2]. The arrangement within the laser is shown in Fig. 20.

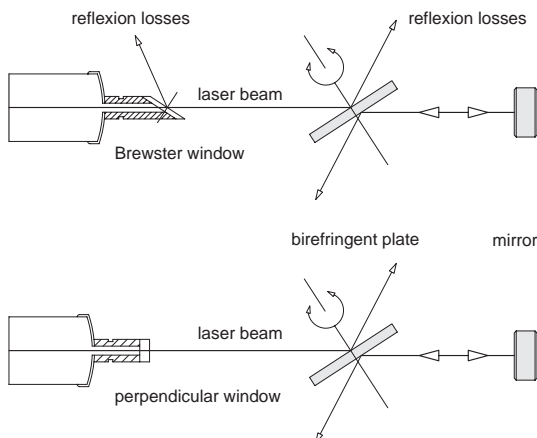


Fig. 20: Birefringent filter for wavelength selection inside the resonator

The birefringent plate is placed under the Brewster's angle into the resonator of the He-Ne laser to avoid reflection losses through the plate itself. The laser can only oscillate in a direction of polarisation given by the Brewster's window or in case of the use of perpendicular windows in the direction of polarisation given by the birefringent plate itself. The birefringent plate does not change the polarisation if a phase shift of  $\delta = 2\pi$  occurs between the ordinary and extraordinary beam after passing through it twice. In this case there will be no reflection losses at any plate orientated under the Brewster's angle. The polarisation of the returning wave changes at every other value of the phase shift  $\delta$  and there are reflection losses at the Brewster's window where the laser will stop oscillating. The phase shift caused by the plate is calculated as follows. The optical path of the ordinary beam is

$$l_o = d \cdot n_o$$

The path of the extraordinary beam is

$$l_{eo} = d \cdot n_{eo}, \text{ so}$$

$$l_o - l_{eo} = d \cdot (n_o - n_{eo})$$

the phase shift  $\delta$  is :

$$\delta(\theta) = \frac{2\pi}{\lambda} \cdot 2 \cdot d \cdot (n_o - n_{eo}(\theta))$$

After passing through twice, where  $d$  is the geometric path followed by the beam in the plate with thickness  $D$  and  $\theta$  is the angle between the electric field vector of light and the optical axis of the crystal lying in the plane of the plate. When

$$\delta(\theta) = \frac{2\pi}{\lambda} \cdot 2 \cdot d \cdot (n_o - n_{eo}(\theta)) = 2\pi$$

there are no losses at the Brewster's window. This applies to a given wavelength for a particular angle  $\theta$ . Now, the thickness  $D$  and the rotational angle  $\theta$  of a plate must be determined using the Jones matrix formalism and which fulfil the above condition in the wavelength area of visible and infrared beams of the He-Ne laser.

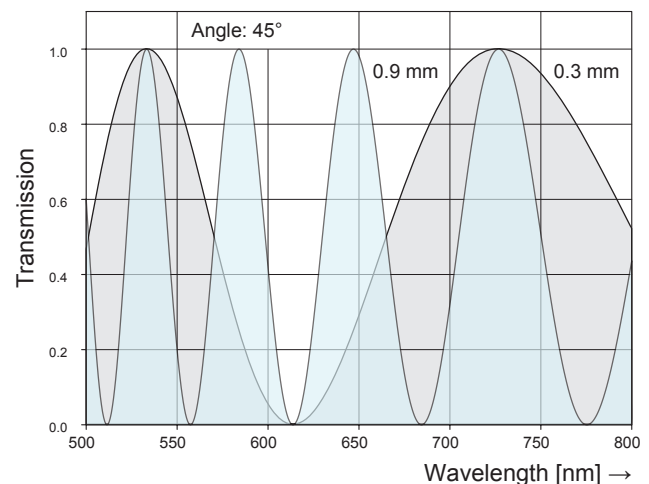


Fig. 21: Transmission of a BFT

Fig. 21 shows the transmission of a plate with a thickness of 0.9 and 0.3 mm, an angle of  $45^\circ$  between the electrical field vector and the optical axis calculated for a wavelength range of 500 - 800 nm

The dispersion of the birefringent quartz was taken into

account in this case. This is why the transmission curves change to higher wavelengths.

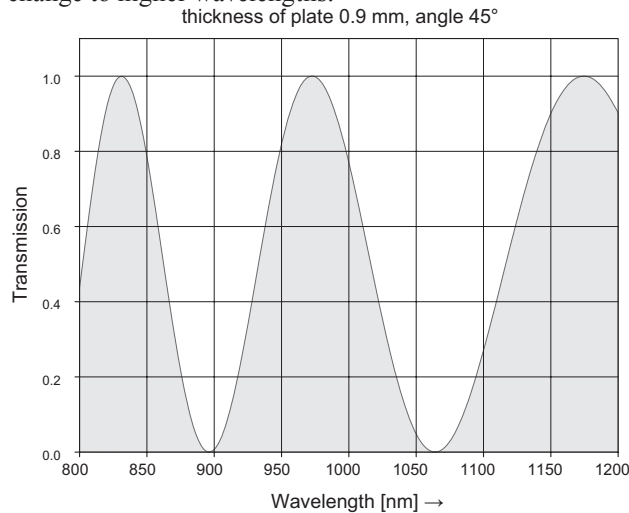


Fig. 22: Calculation as in Fig. 21 but with a wavelength range of 800 - 1200 nm. The transmission curves are wider because of the dispersion.

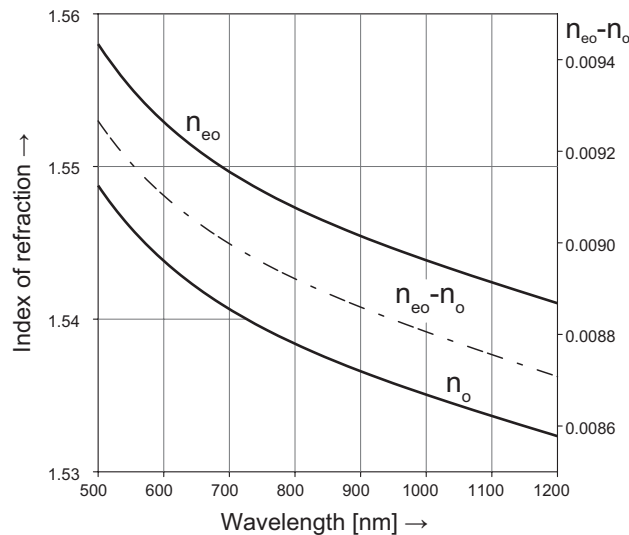


Fig. 23: Dispersion curve for the ordinary and extraordinary refractive index

## 2.6 Mode selection

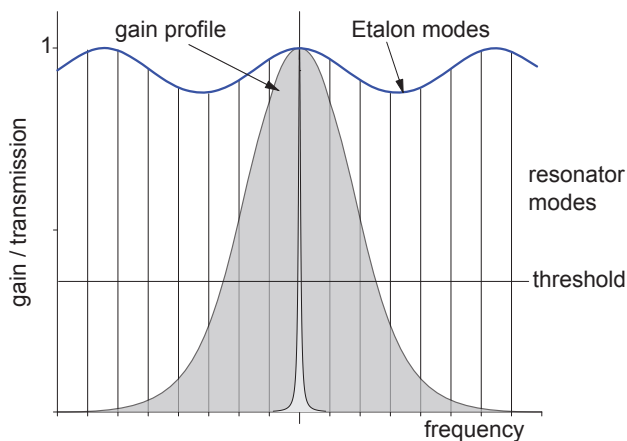


Fig. 24: Mode selection with an etalon

In some areas such as high resolution spectroscopy or interferometric measuring techniques several modes in the laser light prove to be very disturbing (coherence length). Selective frequency losses can be brought into the

resonator by an etalon and undesirable modes are damped and suppressed in this way.

An etalon is a plane parallel, low quality resonator. The etalon usually consists of an individual glass body whose plane surfaces are well ground and polished, parallel to each other.

Just like a normal resonator, an etalon also has modes. However, its modes are considerably broader since the reflection on the plane surfaces is kept low.

If the etalon is tilted by the angle  $\gamma$  against the incoming beam the maximum transmission will change according to:

$$\lambda_m (T = 1) = \frac{2 \cdot d}{m} \cdot \sqrt{n^2 - \sin^2(\gamma)} \quad \text{Eq. 2.7}$$

In this case  $m$  is the  $m$ -th order,  $d$  the thickness of the etalon,  $n$  is the refractive index and  $\gamma$  the tilt angle.

According to Eq. 2.7 the etalon modes can be shifted by tilting the etalon while of course the amplification profile and the resonator modes stay the same. In this way it is possible to encounter more losses in modes that oscillate due to the threshold value amplification than in modes lying just below the maximum transmission.

As in the case of a simple resonator, the distance between the modes is given by the thickness  $d$  and the refractive index  $n$ :

$$\Delta v = \frac{c}{2nd}$$

The etalon must be designed according to the degree of suppression imposed on neighbouring modes and the spectral distance between them. In the HeNe experimental laser used in the following experiments the etalon is 1 cm thick and does not have any additional coating but only 4% reflection on each side due to the Fresnel losses.

## 2.7 Bibliography

*B. Struve, W. Luhs, G. Litfin*, Crystal optics and its importance in laser technology, Year book for optics and precision mechanics 1989

*W. Luhs, B. Struve, G. Litfin*, Tunable multi lines He-Ne laser, Laser and optoelectronics, 4. 1986, AT-Fachverlag GmbH Stuttgart

### 3.0 Experiment

The experiments start with adjusting the basic set up. This is described in the appendix from page 1 onwards. Once the basic adjusting has been done (see up to page 5 of the appendix), we can begin the first experiment.

#### 3.1 Optical stability

The optical resonator of the He-Ne laser is designed according to the given active material (Ne) and the required beam quality.

The objective is to achieve the best possible beam output in the basic Gaussian mode (TEM<sub>00</sub>).

Generally speaking these are two contradictory requirements since a high power output requires the use of a large volume of the active material, whereas the fundamental mode is restricted to its own volume. This is why the hemispherical resonator has the optimal configuration for the He-Ne laser.

#### 3.2 Gaussian beams

This can be explained by the characteristics of Gaussian beams. The beam radius  $w$  ( $w$  = waist) is a result of the following relationship:

$$w(z) = w_0 \cdot \sqrt{1 + \left(\frac{z}{z_R}\right)^2}$$

$w_0$  is the smallest beam radius at the minimum of the beam waist and  $z_R$  is the Rayleigh length.

$$z_R = \pi \cdot \frac{w_0^2}{\lambda}$$

Fig. 25 shows the relationship between the beam diameter and the length  $z$ .  $z$  points into the direction in which the beam is propagating.

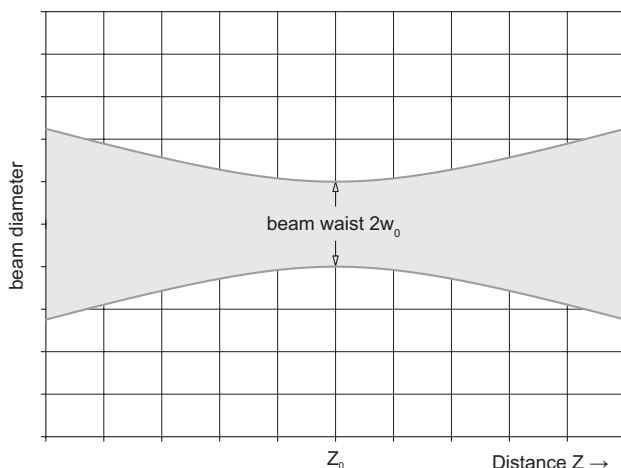


Fig. 25: The beam diameter of a Gaussian beam in the fundamental mode

The beam's radius is smallest at the location  $z_0$ . The beam radius increases in a linear form as the distance increases. Since light waves are spherical waves a radius of curvature of the wave front can be allocated to each location  $z$ . The radius of curvature  $R(z)$  can be calculated with the following relationship:

$$R(z) = z + \frac{z_R^2}{z}$$

This is illustrated in Fig. 26

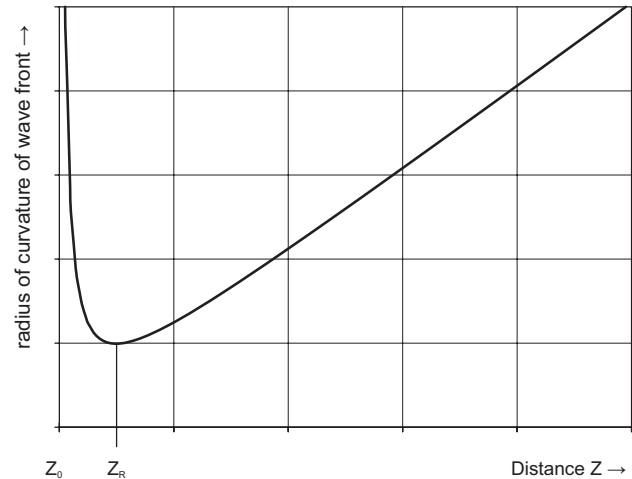


Fig. 26: Radius of curvature of the wave front versus the distance  $z$  from the beam waist at  $z=0$

At  $z = z_R$  the radius of curvature is at a minimum and increases at  $1/z$  against zero. The radius of curvature at  $z=0$  is infinite. At this point the wave front is plane. Above the Rayleigh length  $z_R$  the radius again increases in linear fashion. This is a basic but important statement. It shows that there is a real parallel beam at only one point of the light wave, that is at its focal point. In the range

$$-z_R \leq z \leq z_R$$

a beam can be considered as parallel or collimated. Fig. 27 shows the Rayleigh range as well as the divergence  $\theta$  in the far field.

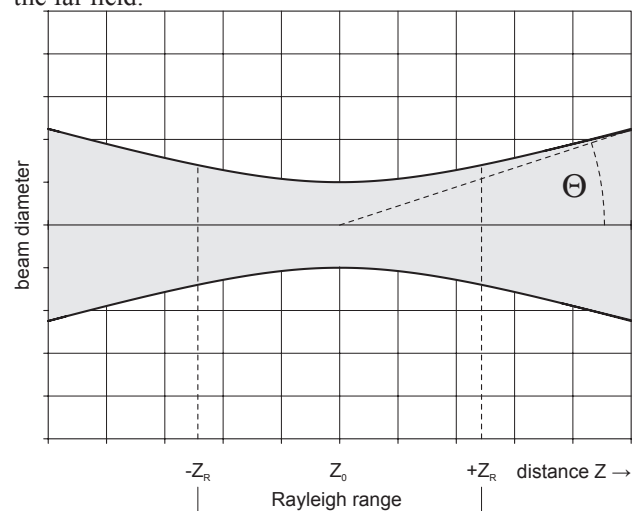
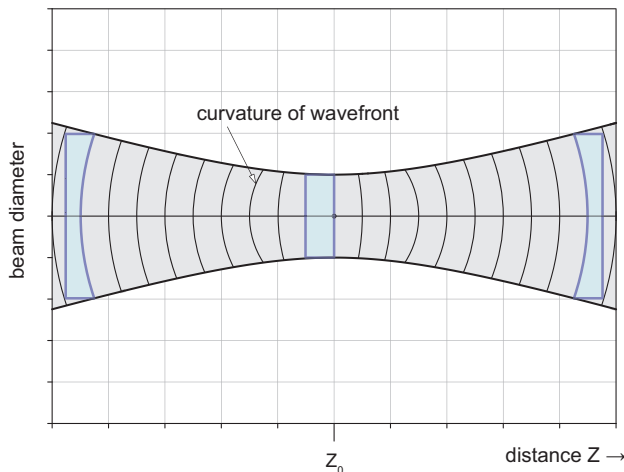


Fig. 27: Rayleigh range and divergence

When reversing the operation a stable optical resonator can now be constructed by adapting the radii of curvature in such a way that they correspond to the radii of curvature of the basic Gaussian mode. This is shown in Fig. 28.



**Fig. 28: Construction of an optical resonator with mirrors. The resonator has the same radii of curvature as the fundamental Gaussian mode has at particular points of  $z$**

Fig. 28 shows a spherical and a hemispherical resonator. If a laser is made to oscillate with this kind of configuration the beam path can be calculated with the above mentioned equations based on the knowledge of the mirror radii and the distance between the mirrors. Due to the demand for a high output power in the fundamental mode, a spherical arrangement is out of question for the He-Ne laser. Transversal modes can also oscillate in spherical resonators. This could also be achieved in this type of resonator by putting up a diaphragm inside the resonator which only allow the fundamental mode to pass freely. However, this option is complicated. The hemispherical resonator is chosen because the place of the plane wave front is very well defined. Only the fundamental mode is reflected back with low losses. Moreover, the He-Ne laser requires a narrow capillary (Chapter 2.1). The recombination process of the laser cycle takes place on its walls. As far as the active material is concerned, the diameter of the capillary should be as small as possible to enable an optimal laser output, but it should not be so small as to block the path of the fundamental mode. The course the beam radius of the mode takes is determined by the radii of curvature and the distance between the mirrors. However, the mode volume, i.e. the volume filling up the fundamental mode, or the length of the amplifying material should be as large as possible to get as much output as possible from the active material. Long tubes are therefore used in He-Ne lasers to increase the output power. At the same time, the radius of the spherical mirror should be big enough for this purpose.

### 3.2.1 Measurements

The objective of the following experiment is the measurement of:

- (1) The optical stability range
- (2) The optical output as a function of the position of the laser tube inside the resonator
- (3) The measurement of the beam radii path inside the resonator.

The measurement (1) will be carried out while the position of the spherical mirror during laser operation is changed up to the stability limit. It can be shifted by slightly loosening the fixing screw on the mirror adjustment support and is still resting lightly on the optical rail. Be careful that the

laser oscillation does not break off due to the shift. The adjustment support is fixed into the new position again and the laser output brought to a maximum by readjustment. Carry on with this until you finally find a position in which no more laser oscillation can be achieved. This position is compared to the maximum distance  $L$  of the mirrors with the radius of curvature  $R$  which can be deduced from the following criteria of stability (see also Eq. 2.5):

$$-1 \leq g_1 \cdot g_2 \leq 1$$

$$g_1 = 1 - \frac{L}{R_1} \quad \text{and} \quad g_2 = 1 - \frac{L}{R_2}$$

The measurement of the output power (2) as a function of the position of the laser tube (capillaries) in the resonator is carried out by loosening the fixing screw on the larger carrier which holds the tube and whose position will be changed. Straight after the first adjustment has been made, it should be ensured that the mechanical axis of the tube corresponds to the optical axis which is defined by the pilot laser. You will notice that the laser output decreases when the position of the tube is brought closer to the spherical mirror. The discussion of the result is based on the beam radius path of the resonator used in consideration of a given capillary diameter. The beam radius path is then measured within the resonator at an optimal position of the laser tube. To measure the beam diameter at a particular position a calliper gauge is used as a measuring diaphragm. The calliper gauge is adjusted to approx. 1.5 mm and placed in the beam path. It is moved back and forth and we then observe whether the laser oscillation returns or not. If it does, the value on the adjusted “diaphragm” is reduced till the laser does not light up any more. The last value at which laser operation was observed is read from the calliper gauge and noted down. This value is the beam diameter at that point. These measurements are repeated at different points and a diagram similar to Fig. 28 should be drawn. Repeat the measurements again but with a clearly changed position of the spherical mirror. Discuss the results taking the thoughts on the path of a Gaussian beam into consideration.

### 3.3 Output power

After carrying out the optimization of the mechanic set-up in the last experiment, we will now measure the influence of the discharge current on the laser output. The output is measured with a photo detector for this purpose. Observe that fluorescent light is also caught by the detector during the discharge. This background must be taken into consideration since only mirrors that transmit very slightly are used for safety reasons. The background is taken with a very slightly de-adjusted resonator to avoid the occurrence of any laser oscillation. The measured background values are subtracted from the following measurement for the different currents in each case. The first series of measurements occurs at the “red line”. After finishing the experiments the same measurements should be repeated for other wavelengths. The dependency found will be discussed in connection with the laser cycle. The desired population of the laser output level and the undesirable population of the laser terminating level play an important role in this case.

### 3.4 Mode structure

Using a lens with a short focal distance (approx. 30-50 mm) the laser's output beam is broadened and mapped on to a screen. The spherical set up of the resonator is used to represent the transverse modes. Higher modes will only be observed by slight de-adjustment. If this does not succeed transverse modes can also be forced. A known characteristic of higher modes is that they have areas where the electric field intensity of light is zero. A "short circuit" of this kind can also be achieved by inserting a thin wire ( even a strand of human hair will do) into the laser beam within the resonator. We can then see a separated distribution of intensities on the screen which look like transverse modes.

### 3.5 Wavelength selection

Wavelength selection is necessary for two reasons. The laser either has undesirable wavelengths due to its specific characteristics or it suppresses wavelengths which only oscillate when a certain wavelength does not oscillate. The latter is true of the visible lines and a part of the infrared lines of the He-Ne laser. Since the visible lines all start from the same level these lines compete with each other. The line with the lowest threshold oscillates first and uses the inversion for its own purposes. Wavelengths with different components can be selected. They are listed below.

#### 3.5.1 Dispersive elements (prisms).

They do not suffer great losses. The separation of lines occurs in two ways. One is through dispersion and the other through geometric length, which is still feasible when carried out between the prism and the laser mirror belonging to it. If the lines are wide apart (approx. 20-30 nm), then distances of 5-10 mm (Littrow prism) are enough for the separation to occur. Lines lying closer together can be separated by a series connection of several prisms. In this procedure a lot of time has to be taken in adjusting, unless an adjustment laser of the same wavelength is available. Due to the Fresnel losses on the surfaces the laser system must have sufficient gain reserves.

#### 3.5.2 Diffractive elements

(Grating). They deviate light in different order with respect to the wavelength. So called Blaze gratings are made in such a way, that the major part of the light is diffracted into the first order. However, the losses for a He-Ne laser are too big.

#### 3.5.3 Interfering elements

(Fabry Perot or etalon, interfering filters). These elements can have very narrow bands but require prefilter since their transmission is repeated periodically. Interference filters seldom reach transmissions of more than 95 %. Etalons are used if modes have to be selected. The etalon itself only has the necessary tuning precision when combined with laser and resonator characteristics.

#### 3.5.4 Elements sensitive to polarisation

(Lyot filter, birefringent filter). Birefringent filters (birefringent tuners) are always used when the laser or the line

to be selected has a defined polarisation (e.g. Brewster surface). If they are put into use under the Brewster's angle they will not suffer great losses. They have periodic transmissions, according to their thickness and wavelength range. They can separate lines lying close to each other without causing any important change in beam direction.

#### 3.5.5 Littrow prism

The basic adjustment is explained from page 24 chapter 4.3 onwards. The Littrow prism is used instead of the plane laser mirror and it fulfils two requirements. It works as a prism for wavelength separation and as a plane laser mirror. Strictly speaking it should be possible to select all the lines of the He-Ne laser for which the coating of the surface of the Littrow prism is suitable. The lines are tuned by tilting the prism. In case the coated surface of the prism directly vertical to the optical axis of the resonator corresponds to the expected laser oscillation the line selected should also oscillate. In fact, this is not the case. We can observe that the dominant "red line" is still oscillating in spite of tilting the prism. However the beam path in the resonator changes (we can observe this at the spherical mirror). The laser beam wanders in the resonator as well, so in spite of the increasing losses, the amplification of the dominant line is sufficient and the others will not be made to oscillate. "Beam walking", an adjustment procedure in which the beam position in the resonator is changed, can be used to push the dominant line to such an extent on the edge of the possible oscillations that the orange line starts oscillating by further tilting of the LPT. "Beam walking" is carried out by slightly turning an adjustment screw on the laser mirror adjustment support and readjusting the output to a maximum by turning the opposite adjustment support in the same direction (x or y). Now the beam changes its direction in the resonator. The iris effect of the capillary stops it from going too far. The objective of the experiment is to understand wave selection with a prism, on the one hand and to get to know the concept of "beam walking" on the other.

#### 3.5.6 Birefringent crystal

From chapter 4.3 on page 23 onwards of the appendix the basic adjustment of the laser with a birefringent tuner (BFT) is explained. The BFT must be set up in the resonator at a place where the laser beam is parallel "as far as possible". The points made on the selective effect of BFT in chapter 2.5.2 on page 10 were based on observations made on collimated beams. If this is not, there would be different angles to the optical axis in the area of a divergent beam. This leads to different phase shifts within the laser beam and thus to a blurring of the polarisation direction. However these effects are comparatively low. Additional losses could therefore be formed for the weak lines, which can be minimised by the optimal position of the BFT within the resonator. If no oscillation of the weak lines can be achieved, the following points must be checked and changed accordingly. All optical surfaces including the surface of the BFT must be well cleaned. The BFT must be adjusted to the Brewster angle to the optical axis. The discharged current should not be more than 5 mA.

### 3.6 Single mode operation with Etalon

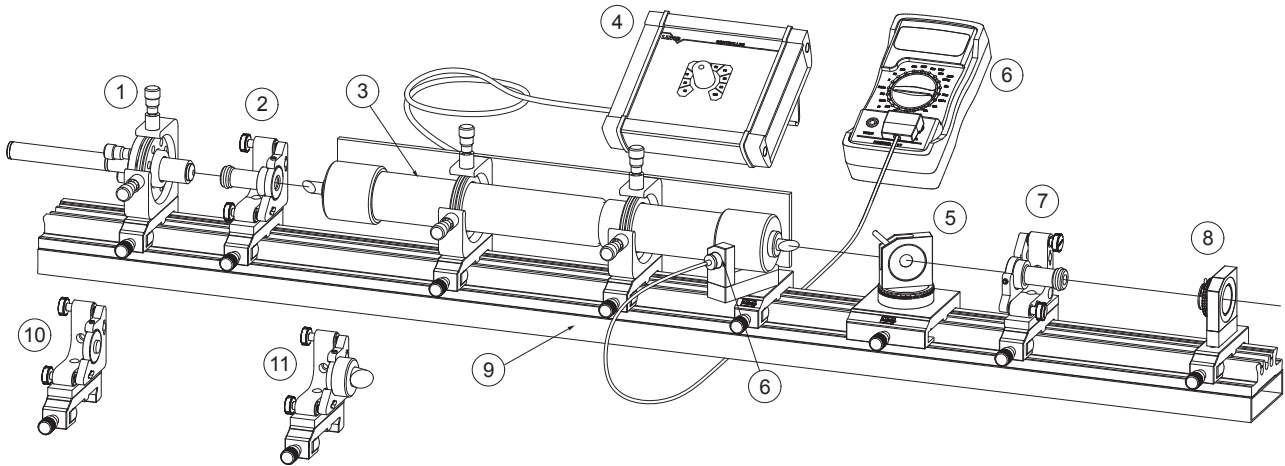
The etalon used is a highly precise quartz glass body produced in a parallel fashion. The thickness is 10 mm and the surfaces are not coated. The etalon is mounted in an adjustment support and can be tilted perpendicularly to the axis of the resonator. The etalon is placed into the well adjusted resonator. Estimating at sight, the etalon is adjusted vertically. After placing the etalon into the resonator the laser should oscillate again. The etalon is now adjusted to the extent that it is vertical to the laser beam. We can observe this in the return reflections of the etalon and in the increased laser output. Now the etalon is at the zero order. By tilting it either horizontally or vertically the laser oscillation is stopped at first and starts oscillating at a particular tilt of the etalon. The first order  $m=1$  has been reached. By tilting the etalon even further higher orders are reached. The output for every arrangement is measured and the result is discussed with reference to the so called "walk off" losses. If a Fabry Perot is available for analysis the single mode operation can be examined. The continuous tuning of the He-Ne laser within its amplification profile will also be observed. The variation in amplitude of the mode while tuning (slight tilting of the etalon) gives you the envelope of the gain profile of Ne.

### 3.7 Operation with infrared lines

Note: Operation with infrared lines is only possible when your system is equipped with a laser tube with Brewster windows. Tubes with perpendicular windows do have an anti reflection coating which is optimised for visible lines only.

The laser mirrors used till now are exchanged for IR mirrors in this experiment. The adjustment is analogous to the basic adjustment when operating with visible lines. Since infrared mirrors have a high transmission for the pilot laser, the return reflexes for adjustment are less, so the room must be slightly darkened when undertaking the initial adjustment. The laser oscillation is first verified with the provided IR-converter screen. The visible fluorescent beam is suppressed with a RG1000 coloured glass filter. The measurements are now carried out analogous to the measurements done to the visible lines. However the Littrow prism cannot be used in wavelength selection since it is only coated for the visible range. The attribution of the BFT selected lines should favourably be done with a monochromator.

## 4.0 Set-Up and description of components



### 4.1 Description of the modules

With the basic set-up the optical resonator will be understood and verified. By means of the provided pilot laser the initial alignment is easy and reproducible.

By changing the distance of the cavity mirrors to each other, the optical stability criterion can be verified and the optimum output power determined. By means of a simple sliding calliper the diameter of the intra-cavity beam can be measured and discussed with respect to Gaussian beams.

When the mechanism of excitation and the relevant energy level scheme is learned the operation of the HeNe-laser at different wavelengths is realised in the next step.

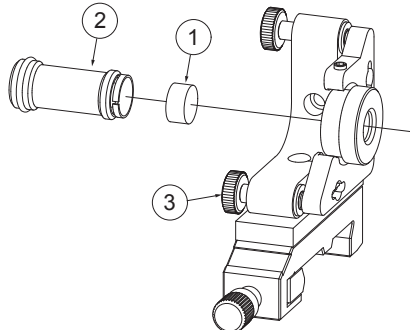


Fig. 29: Module A: Left laser mirror holder (2)

This module contains one resonator mirror (1). It can be screwed out with its fixture (2) from the precise adjustment holder (3). The mirror has a diameter of 1/2 inch and the experiment is supplied with a set of different mirrors.

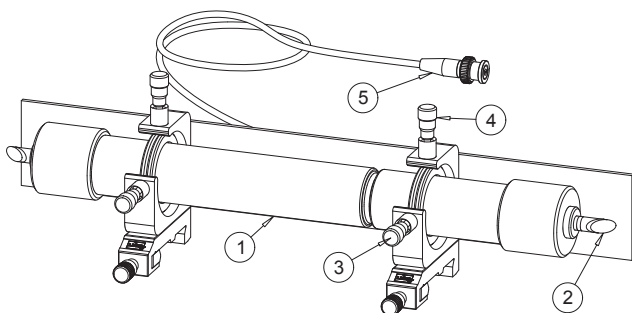


Fig. 30: Module B: Main laser (3)

HeNe-Laser tube with a Brewster's window (2) on both sides mounted in two XY - adjustment holders attached to the back panel. Anode and cathode of the tube are properly

insulated and „touch“-safe. Module B is connected to the controller unit P by means of a high voltage BNC connector (5). The anode of the main laser module is supplied with a voltage of up to 1500 V. Although the metal parts of the laser anode are insulated, cleaning of the laser window should only be done when the tube controller is switched off. Wait for 5 minutes before starting the cleaning process. If the tube is cleaned once before starting the experiments, it is sufficient for several hours.

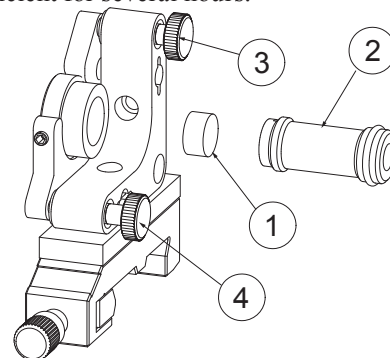


Fig. 31: Module D: Right laser mirror holder (7)

This module contains the other resonator mirror (21). It can be screwed out with its fixture (2) from the holder (3). The mirror has a diameter of 1/2 inch and the experiment is supplied with a set of different mirrors.

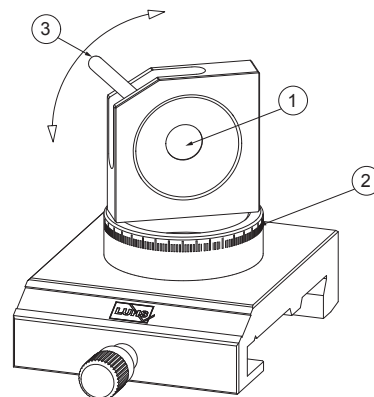
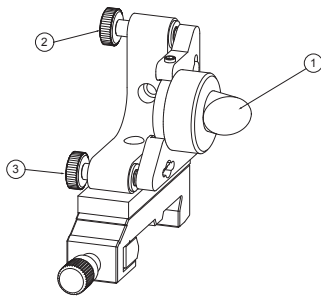


Fig. 32: Module C: Birefringent tuner (5)

A plate of natural birefringent quartz (1) is mounted into a rotator which allows the turning of the plate (3) for tuning different lines of the main laser. With an additional rotator (2) the plate can be tuned precisely to the Brewster's angle.



**Fig. 33: Module G: Littrow's prism tuner (11)**

A high quality Quartz Littrow's prism (1) is supplied with a high reflectivity (>99,98 %) coating covering the range of visible lines of the HeNe laser above 580 nm. The prism is mounted into a precise adjustment holder in such a way that the prism can be aligned with respect to the Brewster's angle of the laser tube. By using the fine pitch screw (3) the prism is tilted for line tuning.

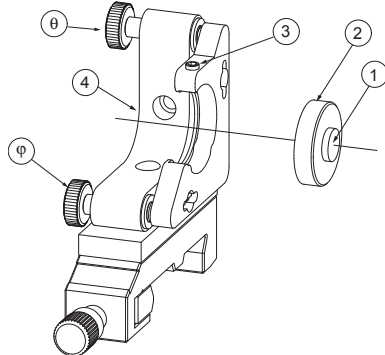


**Fig. 34: Module H: Fabry Perot etalon (10)**

The single mode etalon (1) is mounted into a holder (2). Both surfaces of the etalon are protruding about 1 mm the mount for cleaning purposes. The entire assembly is mounted into the two axes adjustment holder (4) and fixed in its position by the fixing screw (3). By means of the fine pitch adjustment screws the etalon can be tilted ( $\varphi$ ,  $\theta$ ). The etalon has a diameter of  $\frac{1}{2}$  inch and a length of 10 mm. No coating is provided, so that the finesse is determined by the Fresnel reflection losses only.

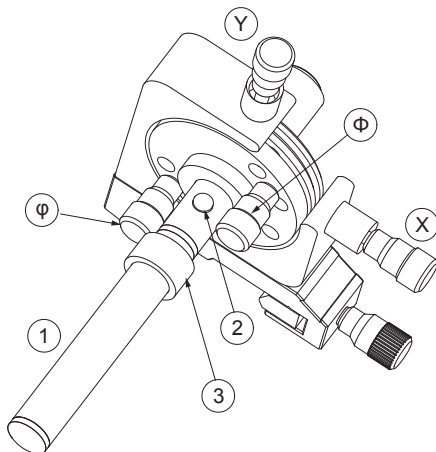


**Fig. 35: Module E: Pilot laser (1)**

The pilot laser (1) consists of a diode pumped solid state laser with frequency doubling emitting a green beam. The output power is about 1 mW. The pilot laser can be shifted in XY as well as tilted in  $\varphi$  and  $\Phi$  direction. The pilot laser is battery operated and the push button (2) is permanently closed by moving the ring (3) over the push button.

Due to the use of high reflective laser mirrors, the output at the mirrors itself is in the range of the transmitted fluorescence light preventing the liable measurement of the laser power. However the light which is reflected from the Brewster's window is much more powerful. Therefore a special photodetector unit is provided for this purpose.

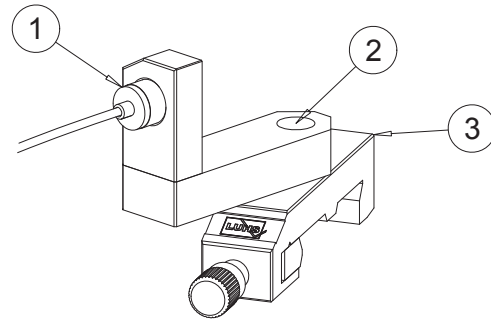


**Fig. 36: Module F: Photodetector (6)**

This unit consists of a Si PIN photodiode accommodated in a housing (1) with attached BNC cable. The detector is connected to the digital multimeter and measures either the relative laser power or when connected to an oscilloscope the beat frequency of the laser modes. The detector is mounted on a radial arm (2) which is set turned to an angle in such a way that the reflected light from the Brewster's window of the HeNe laser tube hits the sensitive area of the detector. The radial arm is screwed to the M6 tread of the carrier (3).

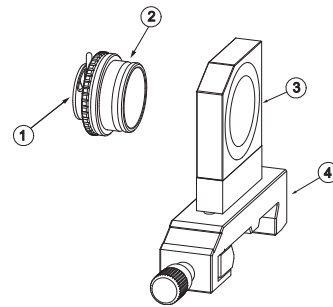


**Fig. 37: Adjustable iris and its mounting plate (8)**

An adjustable iris (1) is mounted in a „click“ - mount (2) to check on the optical axis during the basic adjustment. If required it can be inserted into the mounting plate (3) and placed onto the rail by means of the carrier (4).

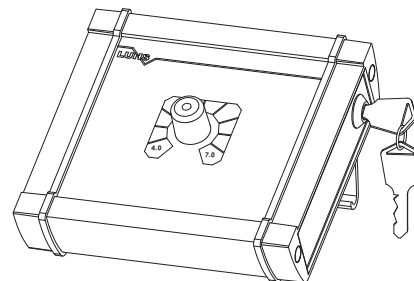


**Fig. 38: Module P: Tube controller (4)**

The tube controller provides the ignition and operation voltage of the laser tube. The unit is operated by 12 VDC at a current of 1.5 A. It is recommended to use the provided wall power supply capable for 2 A. The tube is connected via a special high voltage BNC connector to the controller. A key switch allows operation only for authorised persons. The discharge current can be set by the switch located on the front panel from 4.5 to 6.75 mA in steps of 0.25 mA.

## 4.2 Basic alignment

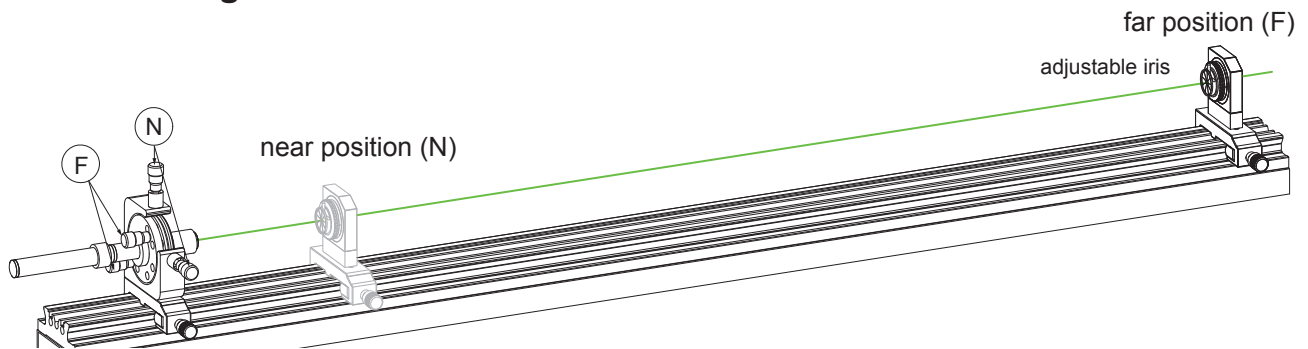


**Fig. 39: Alignment of the pilot laser beam with respect to the optical axis of the optical rail**

The first step is to align the beam of the pilot laser with respect to the centre of the mechanical axis of the set-up. For this purpose the beam is aligned to the centre of the adjustable iris for the nearest and farthest position on the rail. The iris is set to such a diameter that the beam passes with slightly striking it. In the near position (N) the adjustment

screws N are used and in the far position the (F) adjustment screws. The alignment needs three or more iterations to align the beam perfectly in line with the optical axis.

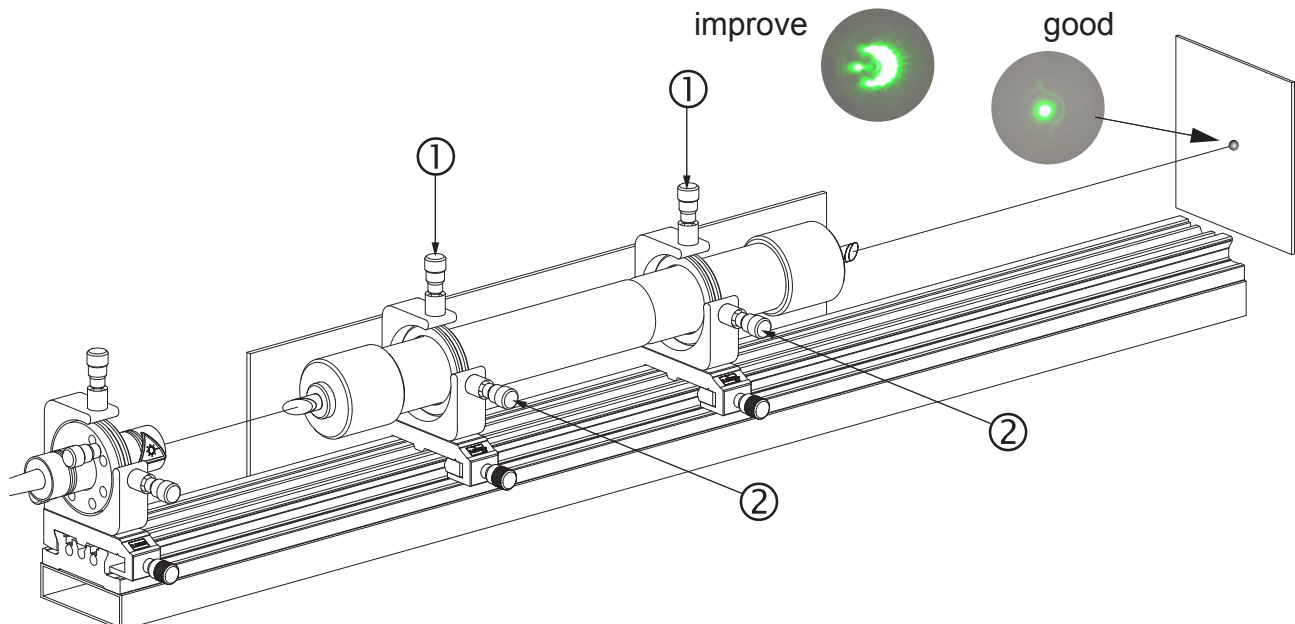


**Fig. 40: Alignment of the laser tube with respect to the pilot laser beam**

Place the main laser onto the rail and fix the clamps. Switch on the pilot laser while the main laser is switched off. The pilot laser has been aligned in the previous step to the optical axis of the set-up and forms also the optical axis of the main laser. Adjust the XY fine pitch screws (1,2) of the tube holder so that the pilot laser beam passes the capillary

of the He-Ne tube without any distortions.

Check the out coming beam by means of a piece of paper. Compare the spot on the paper with the spot of the incoming beam. They must be equal. The better this first tube alignment is, the easier you can align the main laser to oscillation.

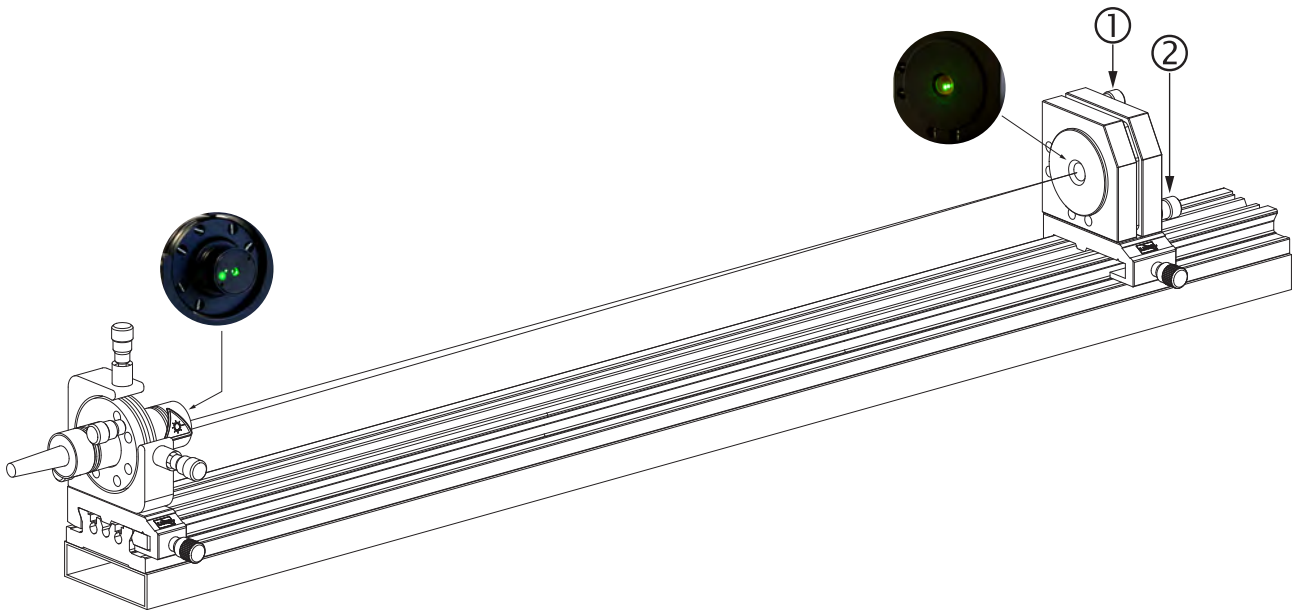


**Fig. 41: Alignment of the right laser mirror**

Place the laser mirror adjustment holder (the right one) onto the rail as shown in the above picture. Use the curved laser mirror with high reflectivity and a radius of curvature of 1000 mm (VIS-1000) and screw it into the holder. Remove the aligned main laser module from the rail. Align the laser mirror in such a way that the reflected laser beam enters exactly the tube of the pilot laser. Observe the back reflected beam on the white screen. When both beams are

centred to each other the laser mirror is well aligned and forms with the resonator of the pilot laser a secondary resonator and interference effects are changing the intensity of the pilot laser beam. This is a hint that the first laser mirror is properly aligned with respect to the optical axis of the pilot laser.

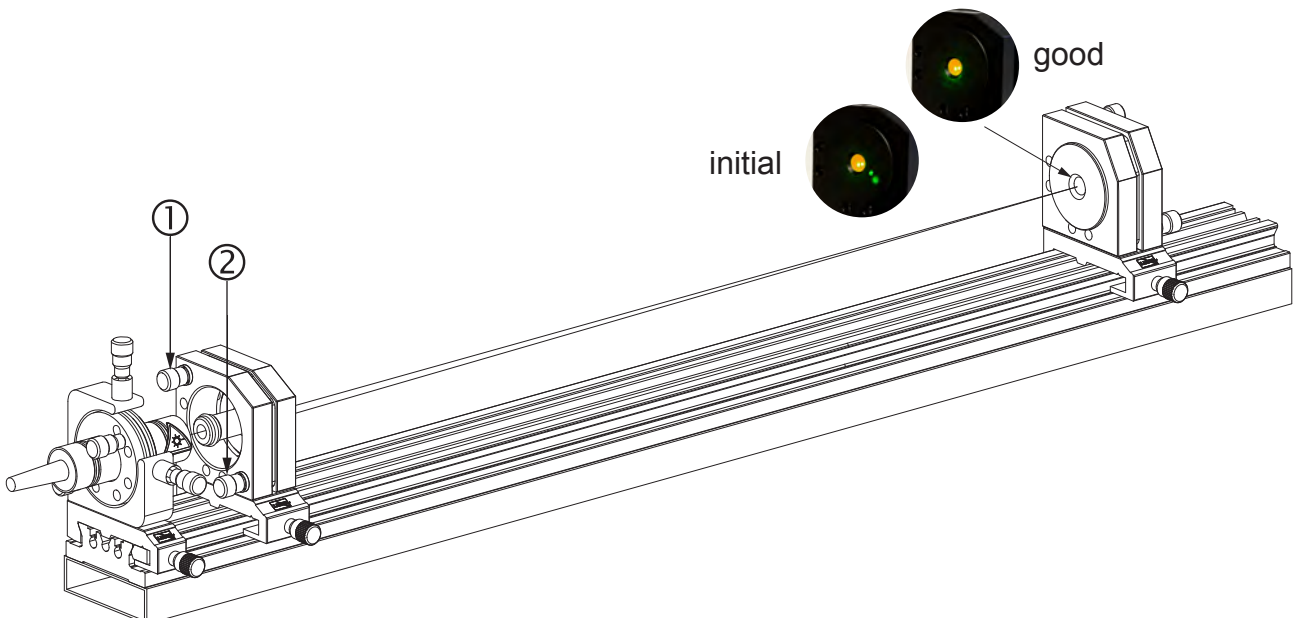


**Fig. 42: Alignment of the left laser mirror**

In the next step the second laser mirror adjustment holder is placed onto the rail as shown above. Use as second resonator mirror that one with the high reflectivity and flat surface (VIS - Flat). Place the mirror holder app. 600 mm apart from the first one. Adjust the back reflected beam in such a way that they are centred on the right laser mirror. The nearer you adjust to the proper position, the more "laser beams" will occur all with increasing divergence.

Centre these beams and you may also observe interference fringes. Note that nearly all laser mirror do have a so called wedge. This means that the plan backside has a small angle deviation with respect to the front side. The wedge shall prevent an unwanted etalon effect. Although the laser mirror aligned by the above described method the front side is not unambiguously aligned properly with respect to the laser axis.

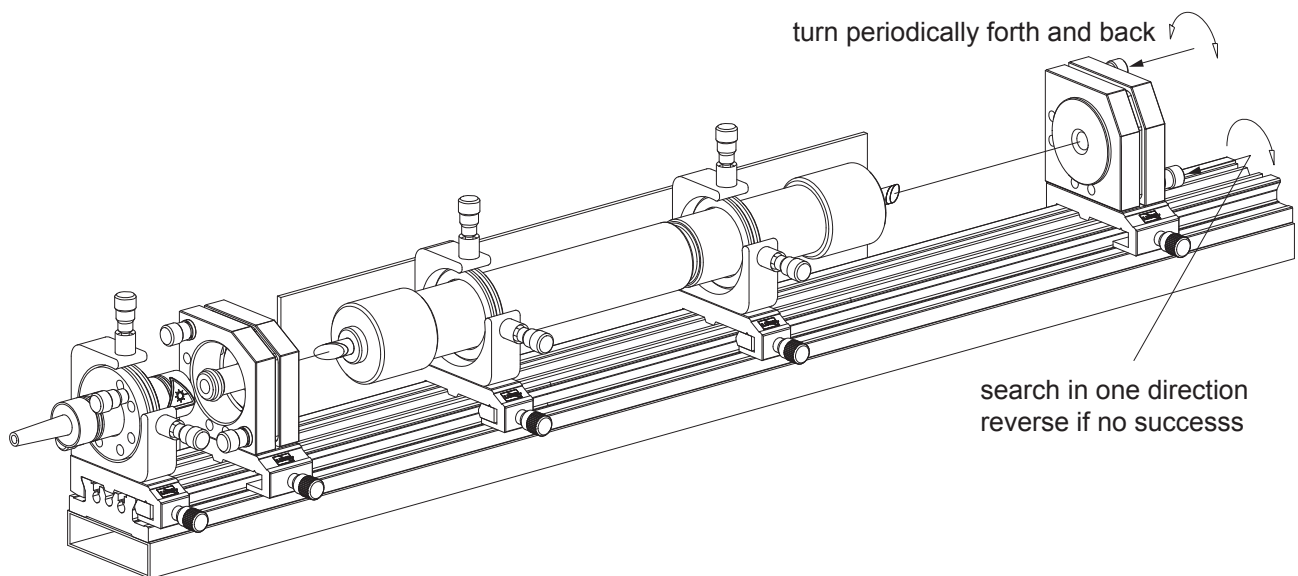


**Fig. 43: Final alignment step**

When all the previous steps are done properly you can now start the main laser to oscillation.

Proceed as following:

Place the tube between the aligned mirrors close to the flat one. Switch the pilot laser off and the main laser on. If the first steps were done properly the laser will start more or less strong immediately.

When not, note the position in mind of the upper adjustment screw and wobble it a little bit. You should observe now flashing up of the laser.

If this fails, we will scan for the proper alignment in such a way that the upper adjustment screw is turned slowly periodically forth and back. While this scan we gently turn the other adjustment screw slowly into one direction. If still no laser oscillation occurs, reverse the rotation direction.

When no other reasons for failure are existing the laser should now show flashing when wobbling the screw. In this case turn the screw to stable oscillation. Realign the upper screw for highest laser power. Realign the left mirror holder for best output.

If still no lasing action will occur, do not waste your time and start the alignment process from the beginning. Because now all components are pre-aligned, this will be done in a few minutes. Make sure that all optics are cleaned and you are using the right mirrors !

### 4.3 Alignment of the birefringent Tuner

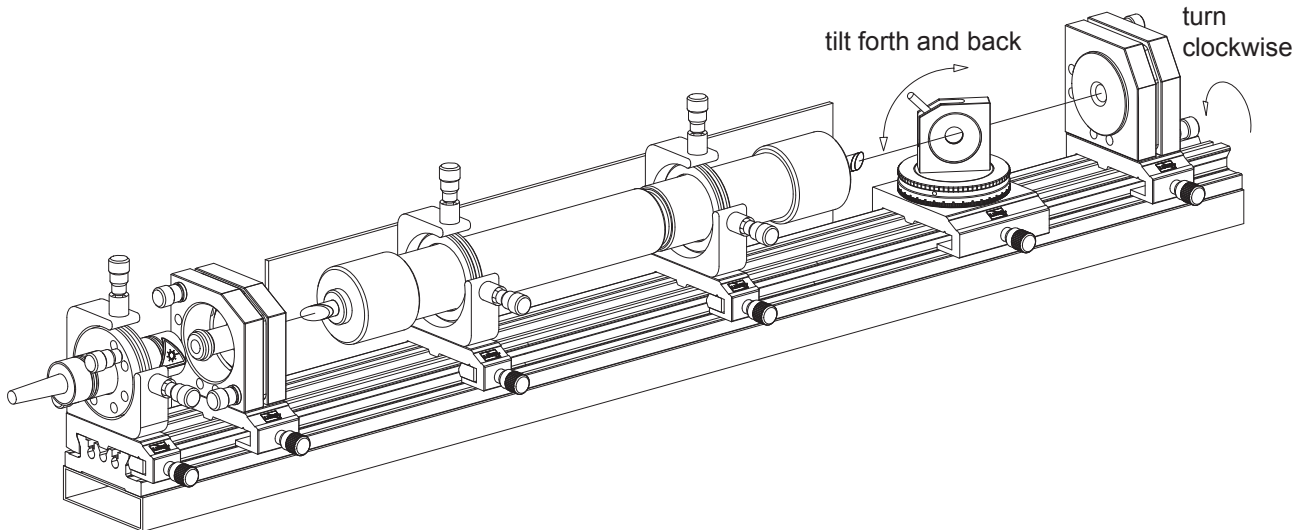


**Fig. 44: Alignment of the birefringent tuner (BFT) see also the instruction movies**

The tuning element consists of a natural quartz plate approx. 1 mm thick. When the BFT is placed into the resonator it causes a beam displacement. Therefore it is necessary to repeat the primary alignment when the tuner is used. It is also possible to insert the tuner into the resonator without carrying out the primary alignment.

Proceed as following:

Align the laser to highest power. Insert the BFT which is already set to the Brewster's angle. Tilt the lever forth and back while gently turning the lower left adjustment screw clockwise. Once laser operation started, tune the BFT and the right laser mirror to the maximum power.

The proper Brewster' angle for the BFT plate also can be found by gently turning the plate holder until the intensity of the reflected beam from the BFT plate shows a minimum. If now the plate is rotated around its optical axis the main line (632.8 nm) will occur 3 to 4 times. Select the best one and realign the laser for best operation.

exposed to pollution because the electrical field of the laser beam on their surfaces is not zero as on the mirrors. Once the orange line is oscillating realign the laser resonator and optimise the Brewster angle by turning slightly the BFT. Note that the line can vanish and will return by tuning slightly the plate.

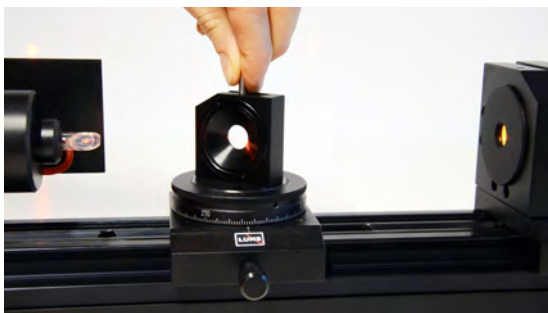


**Fig. 45: Tuning the BFT by tilting the quartz plate**

When you tune in the vicinity of the main line at 632 nm you will find 5 different lines at the following wavelength and relative strength:

1.	611.8 nm	10
2.	629.8 nm	20
3.	632.8 nm	100
4.	635.2 nm	6
5.	640.1 nm	34

The orange line at 611.8 nm as well the line at 635.2 nm are sensitive to additional losses due to pollution on the optics. Clean them again when you will not find these lines. Especially the windows of the tube and the BFT plate are



**Fig. 46: Cleaning the Brewster window of the laser tube**



**Fig. 47: Cleaning the BFT plate from both sides with a special formed cleaning pad**



**Fig. 48: Small cleaning pad**

### 4.4 Alignment of the Littrow Prism Tuner

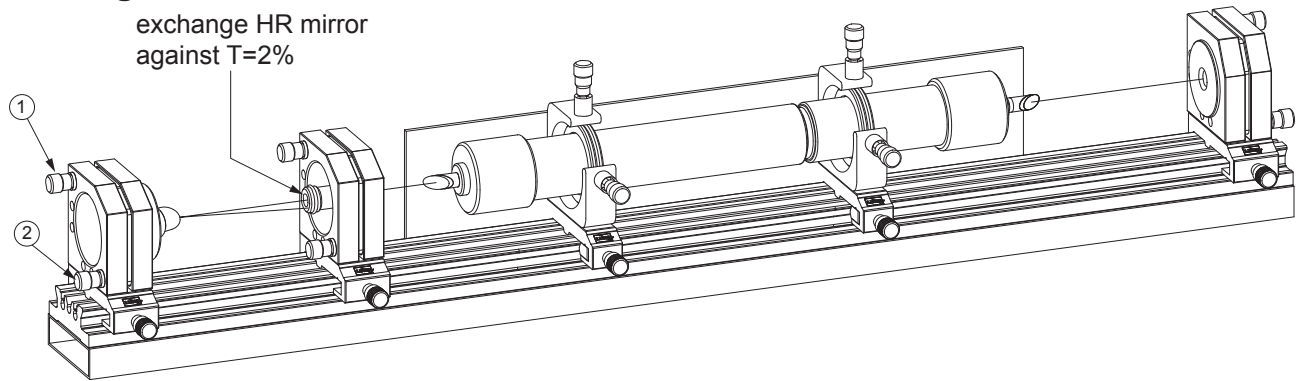


**Fig. 49: Alignment of Littrow's prism**

The Littrow's Prism Tuner (LTP) is a combined optical component consisting of a prism and a reflecting coating. It acts as laser mirror and selective element simultaneously. To align the prism we are placing the module just behind the left laser mirror module as shown above.

travels back in the same direction.

This can be monitored by observing the reflected spots (Fig. 50).

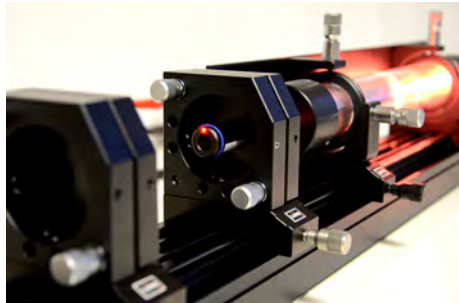


**Fig. 50: Back reflex from the Littrow's prism**

In order to have sufficient light for the alignment the VIS FLAT mirror is exchanged against one with a transmission of 2%. The laser light is reflected by the Littrow's prism. The prism is aligned perfectly when the reflected light

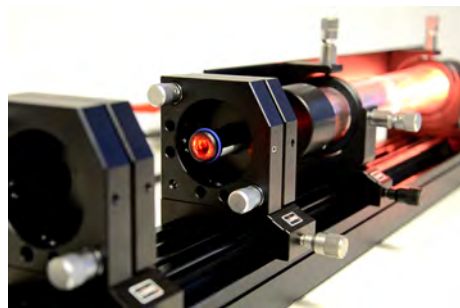


**Fig. 51: Well aligned back reflections**

Beside the dominant beam you will notice a variety of other reflected beams. Centre them all to the main spot. Now you may remove the left laser mirror and if the main laser does not oscillate immediately wobble the laser mirror adjustment screws 2 a bit. Once the laser is started adjust for best operation.

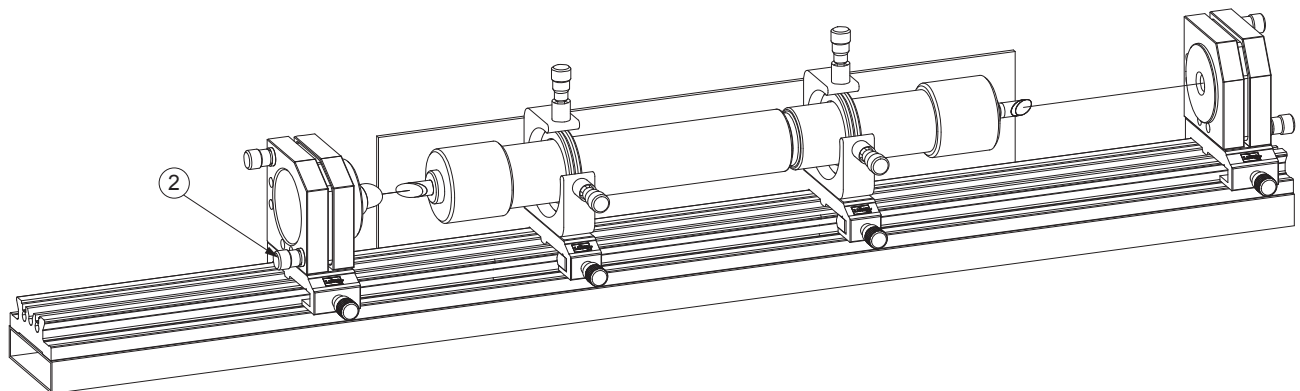


**Fig. 52: Turn the adjustment screw (2) gently counter clockwise to select the orange laser line**

The lower adjustment screw (2) tilts the prism for the desired tuning. Maybe you are surprised, that at the first try no tuning occurs. When you look to the spot of the laser beam on the right mirror you will observe that the spot is moving when the prism is tilted. The main line does not want to decrease to let other lines run. At this point you will realise the advantage of a BFT for separating narrow lines especially with relative short resonators.

If the orange line cannot be selected make sure that the entire laser is aligned for maximum power and the Brewster's window and the laser mirrors are carefully cleaned.

## 4.5 Alignment of the Fabry-Perot Etalon

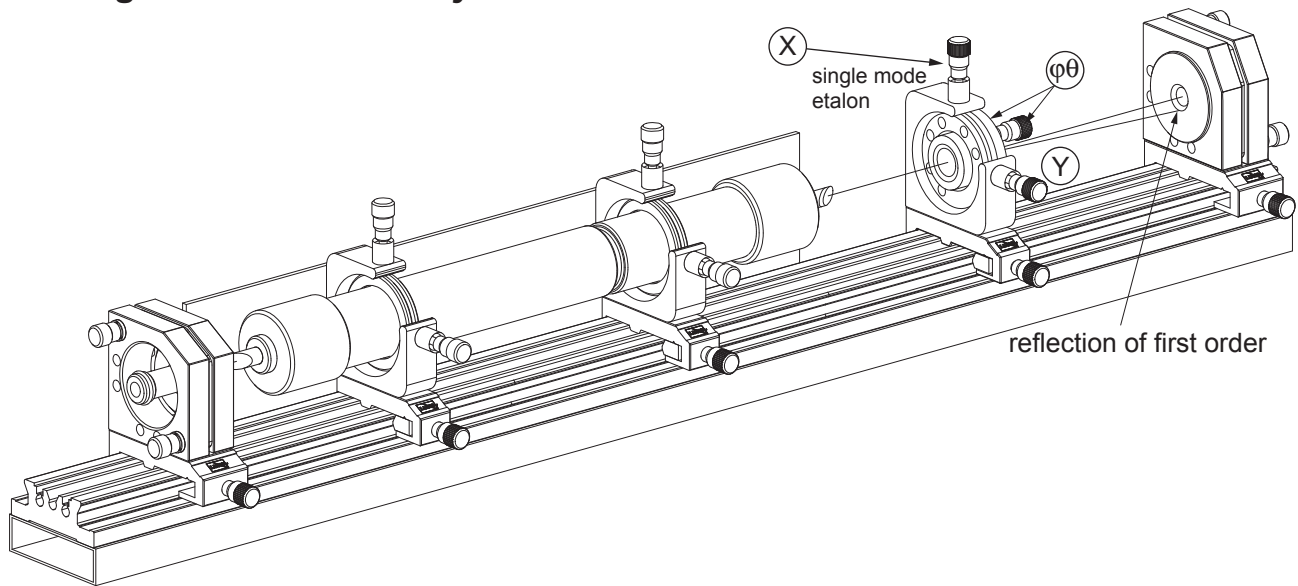


**Fig. 53: Alignment and tuning of the single mode etalon**

Place the single mode etalon module (SM) onto the rail as shown above. The etalon itself consists of a high precision quartz plate with a thickness of 10 mm. The parallel faces are not coated. The Fresnel losses of app. 4% per face are sufficient for the needed Finesse. Before inserting the etalon module make sure that the adjustable part it is aligned parallel to the fixed one. Inspection by sight is sufficient.

In this case the etalon also is aligned perpendicular to the laser axis. Instant more or less strong laser oscillation should occur when the etalon is inserted.

Observe the back reflections of the etalon on the front face of the right laser mirror holder. If the etalon is not aligned perfectly perpendicular (zero order) one will notice several spots.

Align it to the zero order, that means all back reflections must be centred into the main laser beam. With one of the adjustment screws, favourable the upper one, the etalon may now be tilted.



**Fig. 54: Observing the high order reflections of the etalon**

One observes different positions for which laser oscillation again occurs. The check if the laser is running in single mode can be done with an external Fabry Perot, for instance the with the set-up of XP-03 (Fabry-Perot).

If one uses the laser mirror holder of the mentioned experiment with the piezo-electric transducer (PZT) the single mode can also be checked. In addition the observation of the lamb dip is possible.

## 4.6 The high voltage controller ED-0070

The tube controller supplies the main laser with the needed high voltage for ignition and operation. The discharge current of the high voltage supply can be varied in a range from 4.0 to 6.75 mA in order to optimise the laser power for the different lines.

### **Discharge current**

The nominal current of the laser tube is 5 mA. Only for special measurements the laser tube should be used at higher values of the current. By means of the control button, the discharge current can be adjusted between 4.0 and 6.75 mA in steps of 0.25 mA.

### **Key switch**

The key switch located at the side panel prevents unauthorised switching on of the laser.

The controller needs 12 VDC and 2.0 A for its operation. A switched wall plug power supply is provided which is connected via the right panel side.

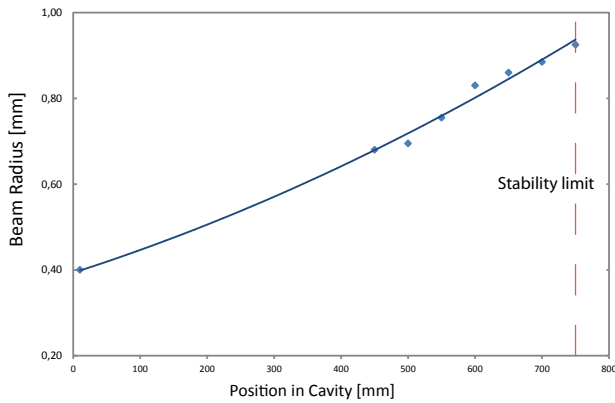
### **Security advices:**

Do not operate the controller without attached laser tube and do not disconnect the tube when controller is switched on!

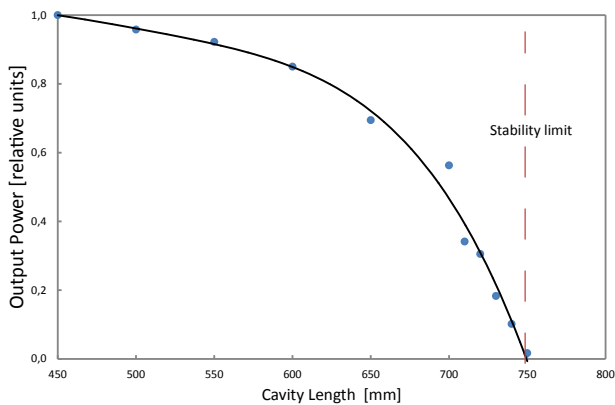


### 4.7 Examples of measurements

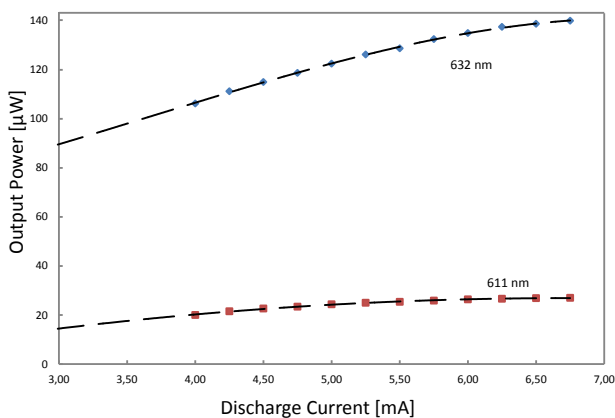
The following graphs show examples of numerical measurements.



By means of a simple calliper used as slit the beam diameter of the intra cavity beam is determined. The above example has been taken with a flat mirror on the left side (zero) and curved mirror (R=750 mm) on the right side.



By using the photodetector the relative output power is determined for the hemispherical cavity with the R=750 mm mirror on the right side. Beyond the stability criterion of 750 mm no more laser oscillation can be observed.



This measurement shows the output power as function of the discharge current. The power has been converted from the reading of the photocurrent into power by using the specific conversion of 0.8 W/A of the provided detector.





[WWW.LD-DIDACTIC.COM](http://WWW.LD-DIDACTIC.COM)



LD DIDACTIC distributes  
its products and solutions  
under the brand LEYBOLD

**LEYBOLD®**